# NADH-driven poly-3-hydroxybutyrate accumulation in Escherichia coli

## Data from enzymatic assays and oxygen-limited continuous cultures

Olavarria, Karel; Quakkelaar, Caspar; van Renselaar, Joachim; Langerak, Dennis; van Loosdrecht, Mark C.M.; Wahl, S. A.

**DOI**
10.1016/j.dib.2020.106588

**Publication date**
2020

**Document Version**
Final published version

**Published in**
Data in Brief

**Citation (APA)**
Olavarria, K., Quakkelaar, C., van Renselaar, J., Langerak, D., van Loosdrecht, M. C. M., & Wahl, S. A. (2020). NADH-driven poly-3-hydroxybutyrate accumulation in Escherichia coli: Data from enzymatic assays and oxygen-limited continuous cultures. *Data in Brief*, *33*, Article 106588. https://doi.org/10.1016/j.dib.2020.106588

Data in Brief 33 (2020) 106588

Contents lists available at ScienceDirect

Data in Brief

journal homepage: www.elsevier.com/locate/dib

Data Article

# NADH-driven poly-3-hydroxybutyrate accumulation in *Escherichia coli*: Data from enzymatic assays and oxygen-limited continuous cultures

Karel Olavarria*, Caspar Quakkelaar, Joachim van Renselaar, Dennis Langerak, Mark C.M. van Loosdrecht, S.A. Wahl

*Departement Biotechnologie, Faculteit Technische Natuurwetenschappen, Technische Universiteit Delft. Van der Maasweg 9, 2629 HZ, the Netherlands*

ARTICLE INFO

*Article history:*
Received 16 November 2020
Revised 20 November 2020
Accepted 23 November 2020
Available online 28 November 2020

*Keywords:*
Acetoacetyl-CoA reductase
Cofactor preference
Polyhydroxybutyrate
Continuous culture
Kinetic characterization
Candidatus Accumulibacter phosphatis
Metabolic fluxes
Data reconciliation

ABSTRACT

Biosynthesis of poly-3-hydroxybutyrate (PHB) as a fermentation product enables the coupling of growth and product generation. Moreover, the reduction of oxygen supply should reduce operative cost and increase product yield. Generation of PHB as a fermentation product depends on the *in vivo* activity of an NADH-preferring acetoacetyl-CoA reductase. Proof of this concept requires (i) quantification of the cofactor preference, in physiologically relevant conditions, of a putative NADH-preferring acetoacetyl-CoA reductase and (ii) verification of PHB accumulation using an NADH-preferring acetoacetyl-CoA reductase in a species naturally incapable of doing so, for example, *Escherichia coli*. This dataset contains kinetic data obtained by spectrophotometry and data from a continuous culture of an engineered *E. coli* strain accumulating PHB under oxygen-limiting conditions. In this dataset it is possible to find (1) enzyme stability assays; (2) initial rates and progress curves from reactions catalyzed by two acetoacetyl-CoA reductases; (3) estimations of the relative use of NADH and NADPH by two acetoacetyl-CoA reductases; (4) estimations of the flux capacity of the reaction catalyzed by an acetoacetyl-CoA re-

DOI of original article: 10.1016/j.jbiotec.2020.10.022
* Corresponding author.
*E-mail address:* k.olavarriagamez@tudelft.nl (K. Olavarria).

https://doi.org/10.1016/j.dib.2020.106588

ductase; (5) biomass composition of an engineered *E. coli* strain transformed with a plasmid; (6) calculation of reconciled specific rates of this engineered strain growing on sucrose as the sole carbon source under oxygen limitation and (7) metabolic fluxes distributions during the continuous growth of this engineered strain. Because a relatively small number of acetoacetyl-CoA reductases have been kinetically characterized, data and scripts here provided could be useful for further kinetic characterizations. Moreover, the procedure described to estimate biomass composition could be interesting to estimate plasmid and protein burden in other strains. Application of data reconciliation to fermentations should help to obtain specific rates consistent with the principle of mass and electron conservation. All the required data and scripts to perform these analyses are deposited in a Mendeley Data repository. This article was co-submitted with the manuscript entitled "An NADH preferring acetoacetyl-CoA reductase is engaged in poly-3-hydroxybutyrate accumulation in *Escherichia*sia. *coli*".



## Specifications Table

| | |
|---|---|
| Subject | Biological Sciences. Biotechnology |
| Specific subject area | Continuous production of poly-3-hydroxybutyrate as a fermentation product under oxygen limitation. |
| Type of data | Figure: Product concentration versus Enzyme concentration times Time.<br>Figure: Initial rates versus acetoacetyl-CoA concentration<br>Figures: Progress curves of reactions catalyzed by acetoacetyl-CoA reductases.<br>Figure: Relative consumption of NADH and NADPH in the reactions catalyzed by two acetoacetyl-CoA reductases.<br>Figure: Flux capacity of a reaction catalyzed by an acetoacetyl-CoA reductase at different $NADH/NAD^+$ ratios.<br>Table: Biomass composition of the *E. coli* strain ((F– λ– *ilvG*– *rfb*-50 *rph*-1 (DE3) Δ*adhE* Δ*adhP* Δ*ldhA* Δ*pta* Δ*mhpF*)) transformed with the plasmid pCOLA-phaCAphaB-cscABK.<br>Table: Non-balanced and reconciled specific rates during the continuous growth of that engineered strain, using sucrose as the sole carbon source, at a dilution rate of 0.1 $h^{-1}$, and oxygen limitation.<br>Table: Metabolic fluxes distributions during the continuous growth of that engineered strain, using sucrose as the sole carbon source, at a dilution rate of 0.1 $h^{-1}$, and oxygen limitation. |
| How data were acquired | In the case of kinetic data, product concentrations were estimated by spectrophotometry and enzyme concentrations were estimated using the Biorad Protein Assay kit. Time and initial rates were automatically recorded/calculated by the spectrophotometer Synergy HTX plate-reader (Biotek) with the software Gen5 (Biotek). Scripts to read and analyze the kinetic data were written and tested with the software DYNAFIT [1] version 4 for Windows (Biokin). Other scripts were written and tested with MATLAB 2020a. |
| Data format | Data from the Selwyn tests are available as Microsoft Excel files where the columns corresponding to Product concentrations and to Enzyme concentration times Time are clearly identified.<br>Data from reaction progress curves are available as .txt files where the first column contains the time (in seconds) and the second column contains the corresponding substrate concentrations (in micromolar).<br>Initial rates are available as a .txt file where the first column contains the concentrations of acetoacetyl-CoA (in micromolar) and the second column contains the initial rates (in micromole of product/micromole of enzyme/second).<br>Data from biomass composition is provided as a Microsoft Excel file. |

(*continued on next page*)

| | |
|---|---|
| Parameters for data collection | Kinetic data were recorded at 30 °C. Continuous cell cultures were studied at 37 °C. Further details are explained in the section Experimental Design, Materials and Methods. |
| Description of data collection | Kinetic data were obtained by spectrophotometry in a plate reader equipped with monochromator, temperature control and a built-in software controlled by the user through the software Gen5. Data from continuous cultures were obtained by the integration of data obtained by different means. More details in the section Experimental Design, Materials and Methods. |
| Data source location | Institution: Department of Biotechnology, Delft University of Technology<br>City/Town/Region: Delft, Zuid Holland<br>Country: Netherlands |
| Data accessibility | Repository name:<br>NADH-driven polyhydroxybutyrate accumulation in *E. coli* dataset 2<br>Data identification number: 10.17632/954dxdncrv.1<br>Direct URL to data: http://dx.doi.org/10.17632/954dxdncrv.1<br>Instructions for accessing these data: Freely available in Mendeley Database. |
| Related research article | Olavarria K., Carnet A., van Ranselaar J., Quakkelaar C., Cabrera R., Guedes da Silva L., Smids A.L., Villalobos P., van Loosdrecht M.C.M., and Wahl S.A.. An NADH preferring acetoacetyl-CoA reductase is engaged in poly-3-hydroxybutyrate accumulation in *E. coli*. Journal of Biotechnology. Accepted on October 18, 2020. https://doi.org/10.1016/j.jbiotec.2020.10.022 |

## Value of the Data

- Open available data from kinetic characterizations of acetoacetyl-CoA reductases are scarce. Here-provided data enable a comparison between the performances using NADH or NADPH. On the other hand, the vast majority of the available PHB accumulation data were obtained in batch. Here we show PHB accumulation rates obtained with continuous cultures, using sucrose as the sole carbon source, and under oxygen limitation.
- The provided data could be useful for colleagues working in artificial operon design, protein engineering, enzyme kinetics, genetic modifications, cell factory design, bioreactor operation and strain physiological characterization.
- The provided data and scripts enable the reproduction of the results reported in the main manuscript linked to this article. Moreover, they also enable to explore different outcomes if the input data is different. For example, NAD(P)(H) concentration ranges, enzyme concentration/activity, kinetic parameters, bioenergetic parameters or biomass composition can be changed.
- Input data and scripts are open and freely available. We provided scripts to perform kinetic parameter estimations, kinetic model discrimination, estimation of cofactor preference, calculation of flux capacity, data reconciliation, elaboration of in silico metabolic models considering plasmid and protein burden. Moreover, we provided DNA sequence maps from different plasmids.

## 1. Data Description

Kinetic data of reactions catalyzed by two acetoacetyl-CoA reductases are presented. One of these enzymes was obtained from a *Candidatus* Accumulibacter phosphatis-enriched mix culture ($AAR^{CAp}$). The other enzyme, $AAR^{Chimera}$, was derived from the acetoacetyl-CoA reductases from *Cupriavidus* necator ($AAR^{Cn}$): the original residues N37-S38-P39-R40-R41 from $AAR^{Cn}$ were replaced by the residues E37-F38-D39-K40-P41 from $AAR^{CAp}$.

The online freely available Mendeley Data repository "NADH-driven polyhydroxybutyrate accumulation in *E. coli* dataset 2″ contains the folder "Enzyme Kinetics data". Inside that folder, it is possible to find the data and conditions from two enzyme stability assays (Selwyn test), performed with $AAR^{CAp}$ (Fig. 1).

Inside the folder "Enzyme kinetics data", it is also possible to find the folder "Data and analysis in DYNAFIT", which contains the following folders:

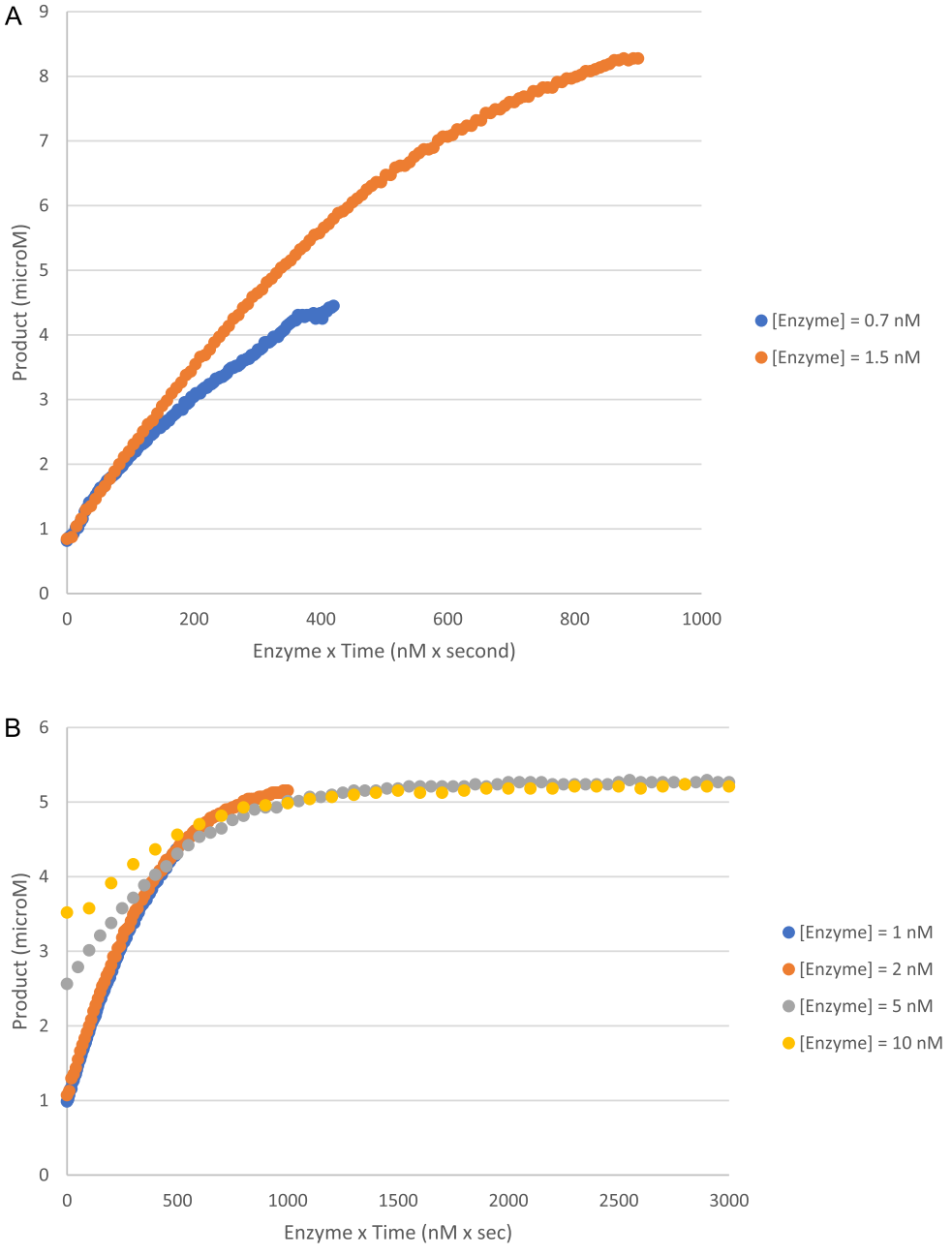


**Fig. 1.** Selwyn plots of reactions catalyzed by $AAR^{CAp}$. Two experiments were performed with different concentration of NADH (A: 10 mM; B: 5 mM). In both experiments, the reaction buffer was 50 mM Tris (pH 8), 5 mM $MgCl_2$, 5 mM NaCl. Temperature was set at 30 °C. Initial acetoacetyl-CoA concentration was 100 mM in both experiments.

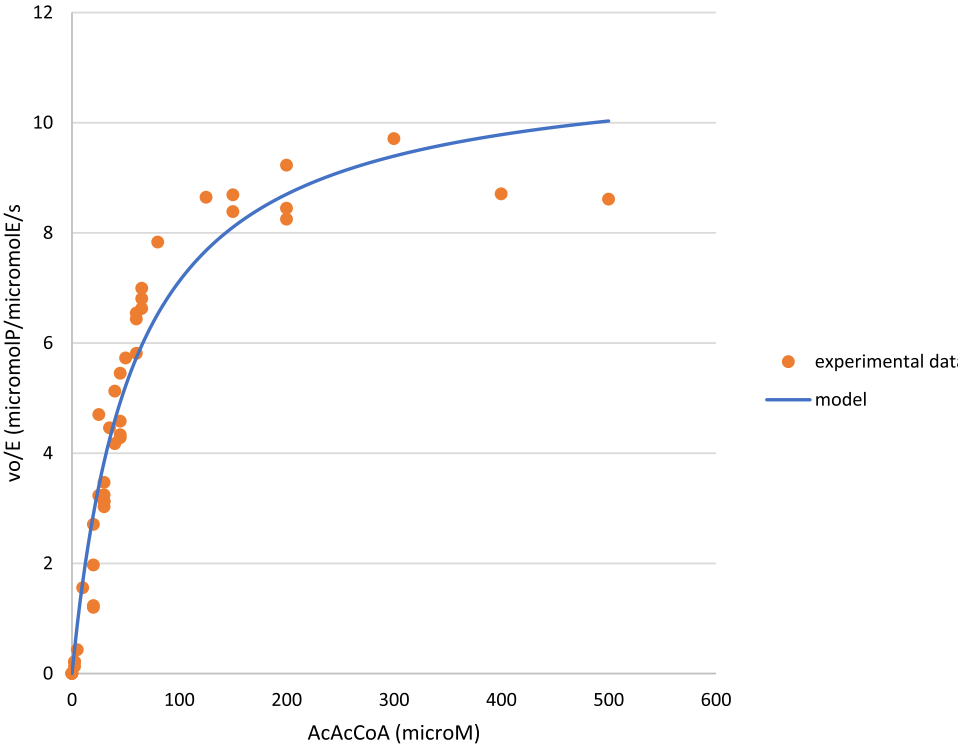


**Fig. 2.** Specific initial rates of reactions catalyzed by $AAR^{CAp}$ at different concentrations of acetoacetyl-CoA. Concentration of the cofactor NADH was fixed at 300 mM. The reaction buffer was 50 mM Tris (pH 8), 5 mM $MgCl_2$, 5 mM NaCl. Temperature was set at 30 °C. Best fit curve was obtained with a simple Michaelian model.

(1) data_AARCAp_varying_AcAcCoA_NADH
(2) data_AARCAp_varying_AcAcCoA_NADPH
(3) data_AARCAp_varying_NADH
(4) data_AARCAp_varying_NADPH
(5) data_AARChimera_varying_NADH
(6) data_AARChimera_varying_NADPH

These folder contains ".txt" files with data from kinetic experiments.

Inside the folder named "data_AARCAp_varying_AcAcCoA_NADH", it is possible to find the file "data.txt". This file contains initial rates of reactions catalyzed by $AAR^{CAp}$, at different concentrations of acetoacetyl-CoA, and NADH concentration fixed at 300 $\mu$M. Data from this experiment are arranged, in the file "data.txt", in two columns. The first column has the assayed acetoacetyl-CoA concentrations (in micromolar) and the second column has the measured initial rates (in micromol of product/ micromol of enzyme/ second) (Fig. 2).

For the other five data folders inside the folder "Data and analysis in DYNAFIT", groups of reaction progress curves are reported. Inside these groups, individual reaction progress curves were reported in separated ".txt" files. Experimental data of reaction progress curves were arranged in two columns. One column has the time (in seconds) and the second column has the varying substrate/cofactor concentration (in micromolar). For each reaction progress curve, the corresponding initial cofactor/substrate and enzyme concentrations are reported in the corresponding ".rtf" file, placed in the same folder "Enzyme kinetics data". These files with the conditions of each assay were named with the format "conditions_XXXXX.rtf". These progress curves were recorded for reactions catalyzed by $AAR^{CAp}$ and $AAR^{Chimera}$. The substrate, cofactor

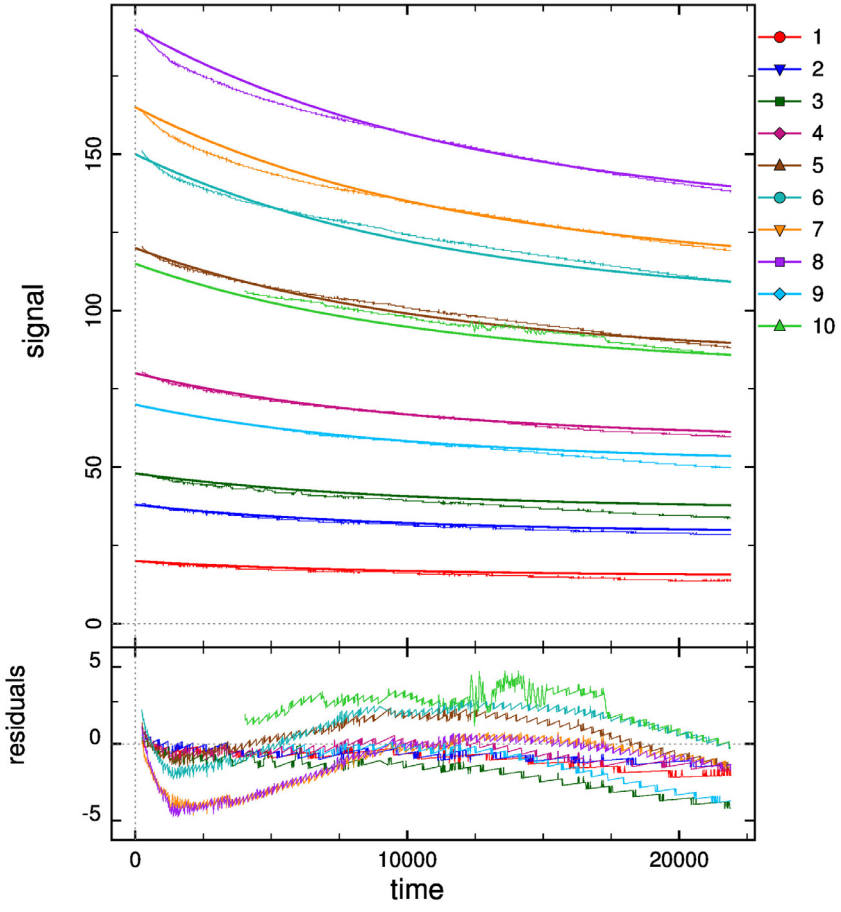


**Fig. 3.** Progress curves of reactions catalyzed by $AAR^{CAp}$ at different acetoacetyl-CoA concentrations. The NADPH concentration was fixed at 300 mM. Time scale is in seconds. The thick lines represent the global fitting, while thinner lines represent the experimental data. Best fit curves were obtained with a simple Michaelian model. The initial concentrations of acetoacetyl-CoA and enzyme were: (1) AcAcCoA = 20 mM, Enzyme = 0.07 mM. (2) AcAcCoA = 38 mM, Enzyme = 0.07 mM. (3) AcAcCoA = 48 mM, Enzyme = 0.07 mM. (4) AcAcCoA = 80 mM, Enzyme = 0.08 mM. (5) AcAcCoA = 120 mM, Enzyme = 0.09 mM. (6) AcAcCoA = 150 mM, Enzyme = 0.1 mM. (7) AcAcCoA = 165 mM, Enzyme = 0.1 mM. (8) AcAcCoA = 190 mM, Enzyme = 0.1 mM. (9) AcAcCoA = 70 mM, Enzyme = 0.08 mM. (10) AcAcCoA = 115 mM, Enzyme = 0.09 mM.

and enzyme concentrations are indicated in each case (Figs. 3–7). The model that best explain each dataset is also indicated in each case. DYNAFIT scripts to analyze the kinetic data are also available in the folder "Enzyme kinetics data".

Inside the folder "Enzyme kinetics data", it is also possible to find a MATLAB script named "Relative_consumption_NADH_NADPH.m". This script enables to calculate and plot the relative use of NADH and NADPH by two acetoacetyl-CoA reductases, at different $NADH/NAD^+$ and $NADPH/NADP^+$ ratios. In the available example, it is possible to make these calculations for the reactions catalyzed by $AAR^{CAp}$ and $AAR^{Cn}$ (Fig. 8). In that calculation, the input data are:

- the equilibrium constant of the reaction catalyzed by the acetoacetyl-CoA reductases (Keq = 92)
- the assumed concentrations of acetoacetyl-CoA (AcAcCoA=22) and 3-hydroxybutyryl-CoA (HBCoA=60) in micromolar.

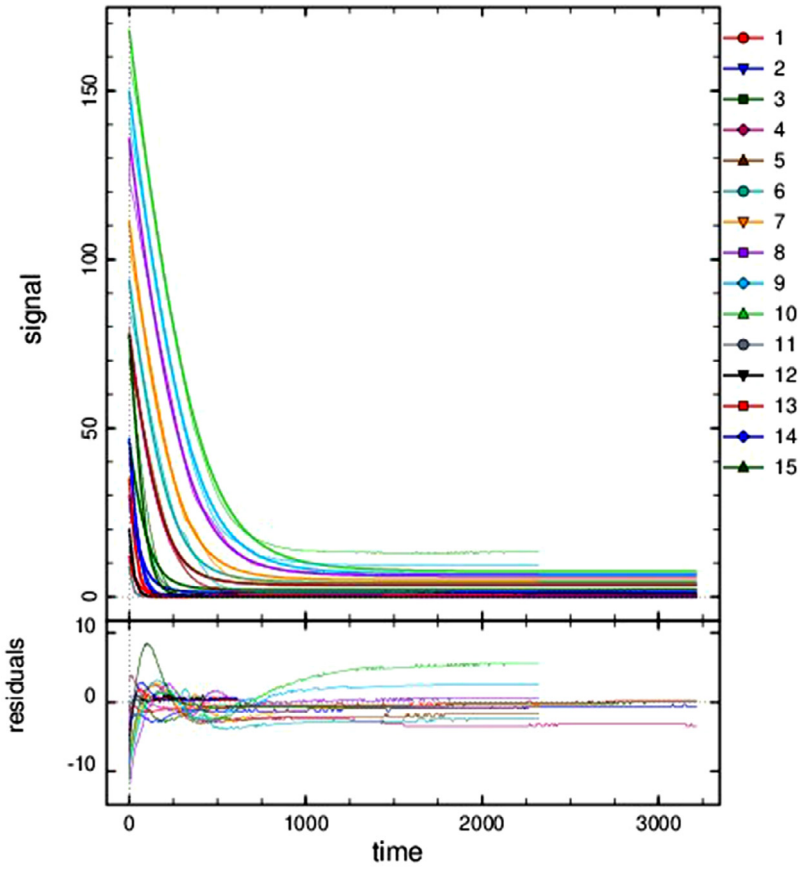


**Fig. 4.** Progress curves of reactions catalyzed by $AAR^{CAp}$ at different NADH concentrations. The acetoacetyl-CoA concentration was fixed at 400 mM. Time scale is in seconds. The thick lines represent the global fitting, while thinner lines represent the experimental data. Best fit curves were obtained with a competitive product inhibition model. The initial concentrations of NADH and enzyme were: (1) NADH = 12 mM, Enzyme = 0.05 mM. (2) NADH = 30 mM, Enzyme = 0.05 mM. (3) NADH = 46 mM, Enzyme = 0.05 mM. (4) NADH = 77 mM, Enzyme = 0.05 mM. (5) NADH = 78 mM, Enzyme = 0.05 mM. (6) NADH = 94 mM, Enzyme = 0.05 mM. (7) NADH = 111 mM, Enzyme = 0.05 mM. (8) NADH = 136 mM, Enzyme = 0.05 mM. (9) NADH = 150 mM, Enzyme = 0.05 mM. (10) NADH = 168 mM, Enzyme = 0.05 mM. (11) NADH = 9 mM, Enzyme = 0.1 mM. (12) NADH = 20 mM, Enzyme = 0.1mM. (13) NADH = 35 mM, Enzyme = 0.1 mM. (14) NADH = 47 mM, Enzyme = 0.1 mM. (15) NADH = 78 mM, Enzyme = 0.1 mM.

- the total sums of $NAD^+$ plus NADH concentrations (moiety_size_NAD) and $NADP^+$ plus NADPH (moiety_size_NADP), in micromolar.
- the more oxidized and the more reduced values for the NADH/$NAD^+$ and NADPH/$NADP^+$ concentration ratios (NADH_over_NAD_ratio_oxidized, NADH_over_NAD_ratio_reduced, NADPH_over_NADP_ratio_oxidized and NADPH_over_NADP_ratio_reduced).
- The main kinetic parameters of the enzymes under comparison.

For the ratios shown in Fig. 8, values of moiety_size_NAD = 1570 [2]; NADH_over_NAD_ratio_oxidized = 0.03 [3], NADH_over_NAD_ratio_reduced = 0.71 [3], moiety_size_NADP = 122 [2] and the extreme values of NADPH_over_NADP_ratio_oxidized = 0.32 [4] and NADPH_over_NADP_ratio_reduced ratios = 60 [2] were used. Regarding the kinetic parameters, they were obtained with the data contained in the folder “Enzyme kinetics data” or obtained from literature. The source of each kinetic parameter is declared in the script.

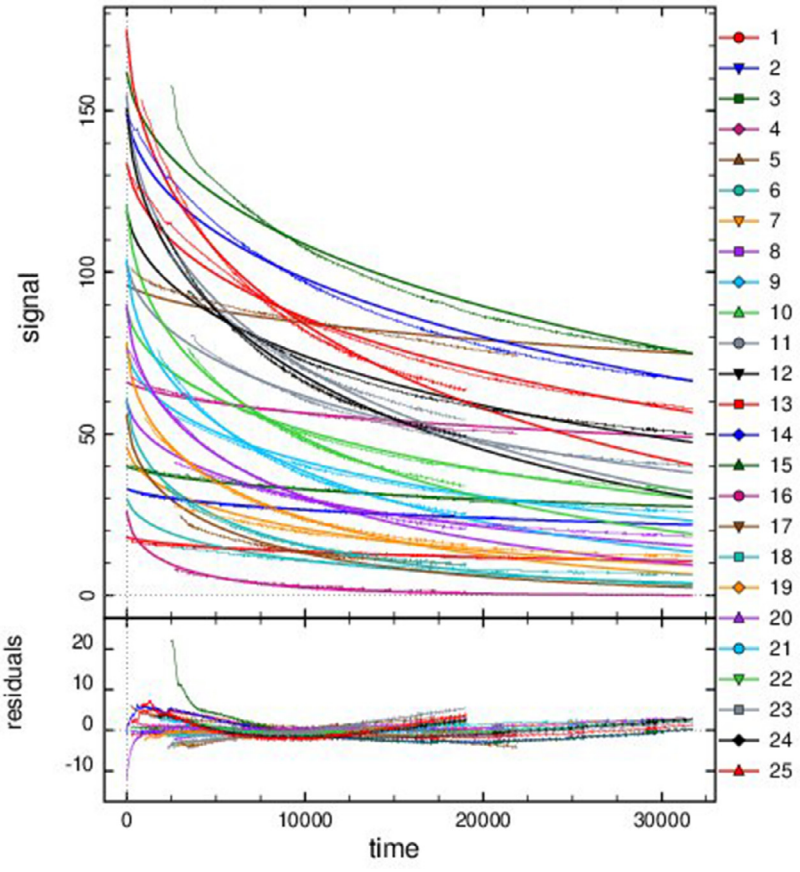


**Fig. 5.** Progress curves of reactions catalyzed by $AAR^{CAp}$ at different NADPH concentrations. The acetoacetyl-CoA concentration was fixed at 400 mM. Time scale is in seconds. The thick lines represent the global fitting, while thinner lines represent the experimental data. Best fit curves were obtained with a competitive product inhibition model. The initial concentrations of NADPH and enzyme were: (1) NADPH = 18 mM, Enzyme = 0.05 mM. (2) NADPH = 33 mM, Enzyme = 0.05 mM. (3) NADPH = 40 mM, Enzyme = 0.05 mM. (4) NADPH = 66 mM, Enzyme = 0.05 mM. (5) NADPH = 96 mM, Enzyme = 0.05 mM. (6) NADPH = 30 mM, Enzyme = 0.5 mM. (7) NADPH = 46 mM, Enzyme = 0.5 mM. (8) NADPH = 60 mM, Enzyme = 0.5 mM. (9) NADPH = 76 mM, Enzyme = 0.5 mM. (10) NADPH = 89 mM, Enzyme = 0.5 mM. (11) NADPH = 103 mM, Enzyme = 0.5 mM. (12) NADPH = 119 mM, Enzyme = 0.5 mM. (13) NADPH = 134 mM, Enzyme = 0.5 mM. (14) NADPH = 149 mM, Enzyme = 0.5 mM. (15) NADPH = 162 mM, Enzyme = 0.5 mM. (16) NADPH = 26 mM, Enzyme = 1.5 mM. (17) NADPH = 56 mM, Enzyme = 1.5 mM. (18) NADPH = 61 mM, Enzyme = 1.5 mM. (19) NADPH = 78 mM, Enzyme = 1.5 mM. (20) NADPH = 90 mM, Enzyme = 1.5 mM. (21) NADPH = 104 mM, Enzyme = 1.5 mM. (22) NADPH = 121 mM, Enzyme = 1.5 mM. (23) NADPH = 155 mM, Enzyme = 1.5 mM. (24) NADPH = 151 mM, Enzyme = 1.5 mM. (25) NADPH = 175 mM, Enzyme = 1.5 mM.

Finally, in the folder “Enzyme Kinetics data”, it is possible to find a MATLAB script to calculate the flux capacity of the reaction catalyzed by $AAR^{CAp}$. Clearly, the same calculation can be applied for another enzyme, provided the corresponding kinetic data be employed as input. This script uses the same input employed to calculate the relative use of NADH and NADPH, plus an estimate of the specific acetoacetyl-CoA reductase activity registered/expected in cells expressing this enzyme. In the specific case shown in the MATLAB script, a specific acetoacetyl-CoA reductase activity of 11.3 nmol/min/mg was employed as input. Convenient conversion factors were introduced in the calculations to express the flux capacity in units of mmol/gCDW/h (Fig. 9).

Beyond the kinetic analyses, in the same Mendeley Data repository “NADH-driven polyhydroxybutyrate accumulation in *E. coli* dataset 2″ it is possible to find a folder named

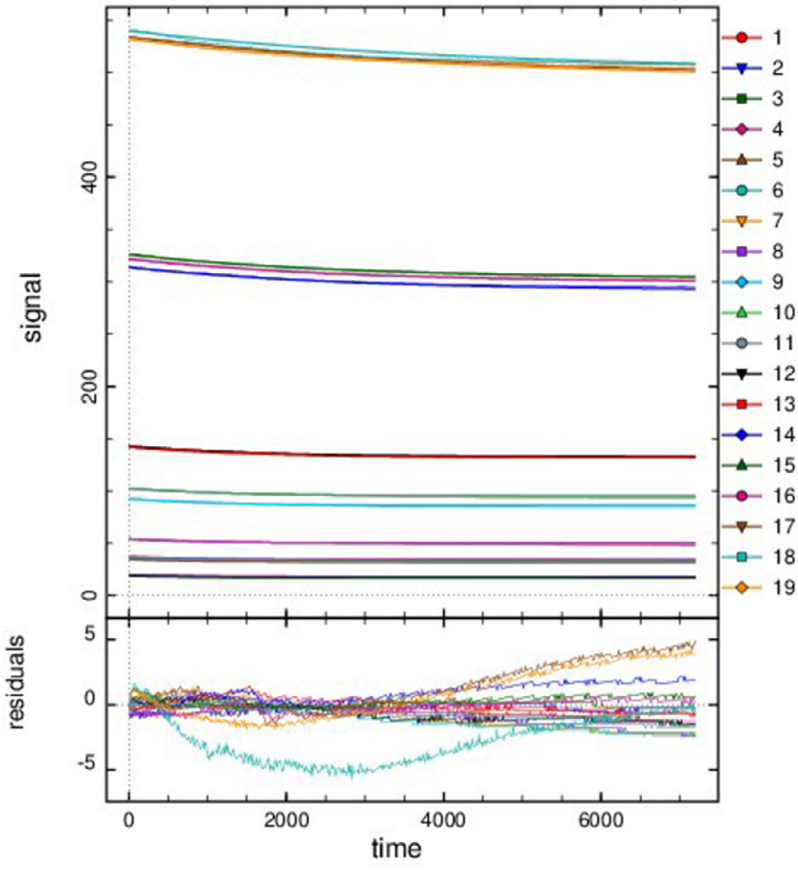


**Fig. 6.** Progress curves of reactions catalyzed by $AAR^{Chimera}$ at different NADH concentrations. The acetoacetyl-CoA concentration was fixed at 400 mM. Time scale is in seconds. The thick lines represent the global fitting, while thinner lines represent the experimental data. Best fit curves were obtained with a simple Michaelian model. The initial concentrations of NADH and enzyme were: (1) NADH = 19.6 mM, Enzyme = 0.002 mM. (2) NADH = 19.4 mM, Enzyme = 0.002 mM. (3) NADH = 18.6 mM, Enzyme = 0.002 mM. (4) NADH = 37.2 mM, Enzyme = 0.002 mM. (5) NADH = 34.6 mM, Enzyme = 0.002 mM. (6) NADH = 36.1 mM, Enzyme = 0.002 mM. (7) NADH = 54 mM, Enzyme = 0.002 mM. (8) NADH = 54 mM, Enzyme = 0.002 mM. (9) NADH = 92.5 mM, Enzyme = 0.002 mM. (10) NADH = 102.5 mM, Enzyme = 0.002 mM. (11) NADH = 102.5 mM, Enzyme = 0.002 mM. (12) NADH = 143 mM, Enzyme = 0.002 mM. (13) NADH = 142 mM, Enzyme = 0.002 mM. (14) NADH = 314 mM, Enzyme = 0.002 mM. (15) NADH = 326 mM, Enzyme = 0.002 mM. (16) NADH = 322 mM, Enzyme = 0.002 mM. (17) NADH = 534 mM, Enzyme = 0.002 mM. (18) NADH = 540 mM, Enzyme = 0.002 mM. (19) NADH = 532 mM, Enzyme = 0.002 mM.

"Fermentations". In that folder, there are different files required to analyze experimental data from a continuous growth of an engineered *E. coli* strain (((F– λ– *ilvG*– *rfb*-50 *rph*-1 (DE3) Δ*adhE* Δ*adhP* Δ*ldhA* Δ*pta* Δ*mhpF*)) transformed with the plasmid pCOLA-phaCAphaB-cscABK). That engineered strain grew with a dilution rate $D = 0.1\ h^{-1}$, under oxygen limitation, and using sucrose as the sole carbon source. Details about how the input information was obtained are described in the section Experimental Design, Materials and Methods. A workflow explaining the interactions among the files present in the folder "Fermentations" is presented in Fig. 10.

Starting with an estimation of the biomass composition (Table 1) and the *in silico* model "Ecolicore.mat" (provided in the repository and also available at the BiGG database, University of California San Diego), the MATLAB script "ModelMaker.m" generates a new *in silico* model (iKOGBurdenD01.mat) with a biomass formation "reaction" including the recombinant DNA and protein burdens (the obtained *in silico* model can be found in the Mendeley Data repository).

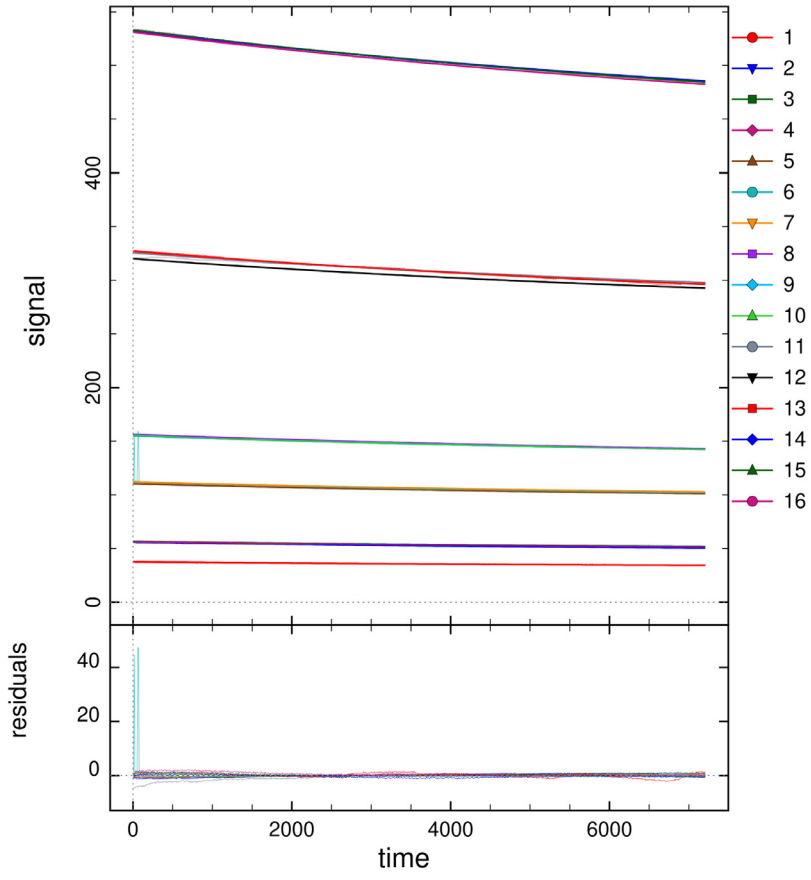


**Fig. 7.** Progress curves of reaction catalyzed by $AAR^{Chimera}$ at different NADPH concentrations. The acetoacetyl-CoA concentration was fixed at 400 mM. Time scale is in seconds. The thick lines represent the global fitting, while thinner lines represent the experimental data. Best fit curves were obtained with a simple Michaelian model. The initial concentrations of NADPH and enzyme were: (1) NADPH = 38 mM, Enzyme = 0.0015 mM. (2) NADPH = 56 mM, Enzyme = 0.0018 mM. (3) NADPH = 56 mM, Enzyme = 0.0015 mM. (4) NADPH = 56 mM, Enzyme = 0.0015 mM. (5) NADPH = 110 mM, Enzyme = 0.0015 mM. (6) NADPH = 112 mM, Enzyme = 0.0016 mM. (7) NADPH = 112 mM, Enzyme = 0.0015 mM. (8) NADPH = 155 mM, Enzyme = 0.0016 mM. (9) NADPH = 155 mM, Enzyme = 0.0015 mM. (10) NADPH = 155 mM, Enzyme = 0.0015 mM. (11) NADPH = 325 mM, Enzyme = 0.0018 mM. (12) NADPH = 320 mM, Enzyme = 0.0018 mM. (13) NADPH = 327 mM, Enzyme = 0.002 mM. (14) NADPH = 532 mM, Enzyme = 0.0021 mM. (15) NADPH = 533 mM, Enzyme = 0.0022 mM. (16) NADPH = 531 mM, Enzyme = 0.0022 mM.

To run this MATLAB script, the freely available COBRA Toolbox for MATLAB [5] version 2.0 or higher, has to be previously installed.

Once the model iKOGBurdenD01 is constructed, the script “data_reconciliation_plus_FBA.m”, which includes the unbalanced rates (Table 2) manually introduced, can perform a flux balance analysis and generates different output files. COBRA Toolbox is also required to run this script. However, we are also including in the repository a script to perform data reconciliation without the participation of the COBRA Toolbox (data_reconciliation_only). Different output options are available in the script “data_reconciliation_plus_FBA.m”: Balanced (reconciled) rates with their associated errors; optimum, maximum and minimum feasible fluxes (Table 3); a visual representation of the metabolic fluxes and the calculation of the fluxes contributing to the formation and consumption of any given metabolite included in the *in silico* model. Clearly, under steady-state, the sum of the fluxes contributing to the formation of a given metabolite must be equal to the sum of the fluxes consuming that metabolite.

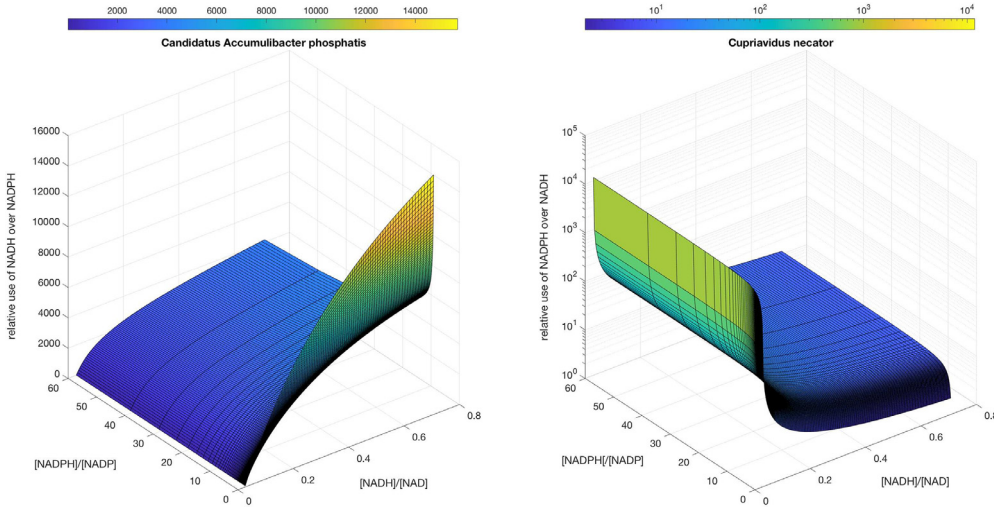


**Fig. 8.** Relative use of NADH over NADPH (or vice versa) by the acetoacetyl-CoA reductases from Ca. A. phosphatis and *C. necator*.

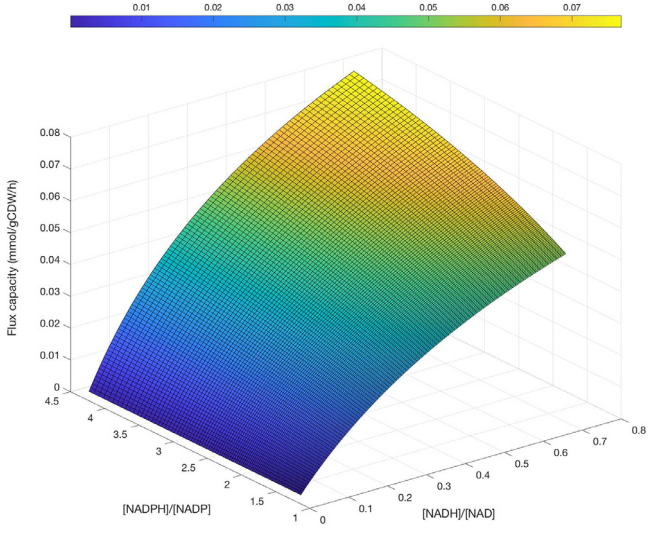


**Fig. 9.** Flux capacity of the reaction catalyzed by $AAR^{CAp}$ at different NADH/NAD+ and NADPH/$NADP^{+}$ concentration ratios.

## 2. Experimental Design, Materials and Methods

### *2.1. DNA manipulations*

For routine procedures, cells were grown on Lysogenic Broth (LB) medium (10 g tryptone, 5 g yeast extract and 5 g NaCl per liter of deionized water) supplemented with *ad hoc* antibiotics. The characteristics of the primers, plasmids and strains employed in this research are summarized a supplementary material of the accompanying paper "An NADH preferring acetoacetyl-CoA reductase is engaged in poly-3-hydroxybutyrate accumulation in *E. coli*".

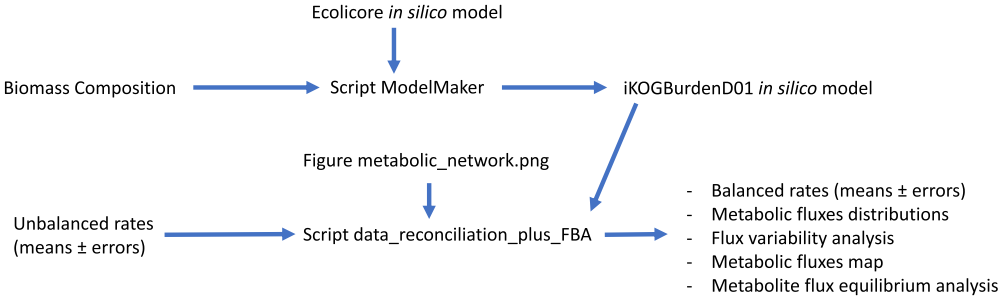


**Fig. 10.** Workflow to reproduce the analysis of the continuous cultures. As output, it will be possible to calculate balanced specific rates, metabolic fluxes distributions, flux variability analysis, generate a metabolic fluxes map and calculate the fluxes contributing to the maintenance of the steady-state of a given metabolite.

**Table 1**
Biomass composition of the engineered strain after considering plasmid and heterologous protein contributions. Relative elemental composition for each component is below the columns identified with the symbol of the elements carbon, hydrogen, nitrogen, oxygen, sulfur and phosphorous. After considering recombinant DNA and protein burdens, 1 carbon-mol of biomass (CmolX) has a "molecular" weight of 23.1840 gCDW/CmolX, and its reduction degree is $\gamma$=4.2920.

| Biomolecules | Percent of weight (%) | C | H | N | O | S | P | mol per CmolX |
|---|---|---|---|---|---|---|---|---|
| Protein | 64.68 | 1.000 | 1.580 | 0.288 | 0.309 | 0.009 | 0.00 | 0.656327 |
| DNA | 1.04 | 1.00 | 1.05 | 0.39 | 0.62 | 0.00 | 0.10 | 0.007682 |
| Ethanolamine | 2.59 | 2.00 | 8.00 | 1.00 | 1.00 | 0.00 | 0.00 | 0.009683 |
| Glycerol | 4.31 | 3.00 | 8.00 | 0.00 | 3.00 | 0.00 | 0.00 | 0.010852 |
| Glycogen | 0.59 | 6.00 | 10.00 | 0.00 | 5.00 | 0.00 | 0.00 | 0.000842 |
| Hexadecanoate | 2.96 | 16.00 | 31.00 | 0.00 | 2.00 | 0.00 | 0.00 | 0.002691 |
| Hexadecenoate | 2.28 | 16.00 | 29.00 | 0.00 | 2.00 | 0.00 | 0.00 | 0.002086 |
| Lipopolysaccharide | 0.81 | 171.00 | 297.00 | 4.00 | 88.00 | 0.00 | 2.00 | 0.000048 |
| Octadecenoate | 1.65 | 18.00 | 33.00 | 0.00 | 2.00 | 0.00 | 0.00 | 0.001362 |
| Peptidoglycan | 0.59 | 40.00 | 62.00 | 8.00 | 21.00 | 0.00 | 0.00 | 0.000138 |
| Putrescine | 0.28 | 4.00 | 14.00 | 2.00 | 0.00 | 0.00 | 0.00 | 0.000709 |
| RNA | 6.89 | 1.00 | 1.02 | 0.41 | 0.73 | 0.00 | 0.10 | 0.047476 |
| Spermidine | 0.09 | 7.00 | 22.00 | 3.00 | 0.00 | 0.00 | 0.00 | 0.000149 |
| Heterologous proteins | 5.02 | 1.00 | 1.58 | 0.29 | 0.31 | 0.01 | 0.00 | 0.050939 |
| Plasmid | 0.13 | 1.00 | 1.05 | 0.39 | 0.62 | 0.00 | 0.10 | 0.000946 |
| Ash | 6.10 | | | | | | | |

DNA amplification, restriction and ligation as well as bacterial transformation, selection and identification were executed according to the standard procedures described elsewhere [6]. When amplifying DNA for cloning purposes, Q5 High-Fidelity DNA Polymerase (New England Biolabs) was used. GoTaq Green Master Mix (Promega) was used for colony PCR. Plasmid purification from cultures was done using the QIAprep Spin Miniprep Kit (Qiagen). For plasmid propagation and long-term storage of constructions, introduction of the plasmids in *E. coli* One Shot® TOP10 (ThermoFisher Scientific) was implemented. All DNA modifying enzymes employed in this study were purchased from New England Biolabs.

$AAR^{CAp}$ is encoded by the $phaB^{CAp}6$ gene. The $phaB^{CAp}6$ gene was isolated from a metagenomic DNA sample obtained from a *Ca.* A. phosphatis-enriched mix culture. This gene has a very high DNA identity with the annotated *phaB* gene from *Ca.* A. phosphatis (locus KEGG CAP2UW1_3919). To amplify and clone $phaB^{CAp}6$ gene, a sample of total DNA from the mix culture was obtained with the commercially available PowerSoil® DNA isolation Kit (MO BIO Laboratories), following the instructions of the manufacturer. The enrichment of that mix culture was done using an enhanced biological phosphorus removal procedure [7], starting with crushed granular sludge from the Garmerwolde Nereda plant, The Netherlands. A sample of the obtained DNA (30 ng) was used as template in a PCR reaction using the primers PAOphaB_BamUpCrt and

**Table 2**
Specific unbalanced and reconciled rates for the engineered strain growing in a continuous culture, under oxygen limitation, using sucrose as the sole carbon source.

| Steady-state 1 | | | | | | | |
|---|---|---|---|---|---|---|---|
| | | Raw data | | unbalanced means | unbalanced SD | renconciled means | reconciled SD |
| $q_x$ ($h^{-1}$) | 0.0978 | 0.0952 | 0.1055 | 0.100 | 0.005 | 0.1098 | 0.0041 |
| $q_{sucrose}$ (mmol/gCDW/h) | −0.718 | −0.6857 | −0.6501 | −0.685 | 0.0343 | −0.7906 | 0.0155 |
| $q_{acetate}$ (mmol/gCDW/h) | 0.0074 | 0.0073 | 0.0042 | 0.0063 | 0.002 | 0.0062 | 0.002 |
| $q_{lactate}$ (mmol/gCDW/h) | 0.0454 | 0.0564 | 0.049 | 0.0503 | 0.006 | 0.0495 | 0.006 |
| $q_{succinate}$ (mmol/gCDW/h) | 0.0467 | 0.0391 | 0.0381 | 0.0413 | 0.005 | 0.0377 | 0.005 |
| $q_{CO2}$ (mmol/gCDW/h) | 4.57 | 4.616 | 4.619 | 4.600 | 0.027 | 4.4285 | 0.0183 |
| $q_{O2}$ (mmol/gCDW/h) | −3.97 | −3.996 | −4.011 | −4.000 | 0.021 | −4.1004 | 0.0174 |
| $q_{PHB}$ (mmol/gCDW/h) | 0.0022 | 0.00219 | 0.0025 | 0.0023 | 0.0001 | 0.0023 | 0.0001 |
| $q_{formate}$ (mmol/gCDW/h) | b.d.l. | b.d.l. | b.d.l. | 0 | 0 | 0 | 0 |
| Steady-state 2 | | | | | | | |
| | | Raw data | | unbalanced means | unbalanced SD | renconciled means | reconciled SD |
| $q_x$ ($h^{-1}$) | 0.1057 | 0.0977 | 0.096 | 0.100 | 0.005 | 0.0939 | 0.0041 |
| $q_{sucrose}$ (mmol/gCDW/h) | −0.8191 | −0.8148 | −0.8231 | −0.819 | 0.041 | −0.6675 | 0.0163 |
| $q_{acetate}$ (mmol/gCDW/h) | 0.1622 | 0.207 | 0.1992 | 0.1893 | 0.024 | 0.198 | 0.0239 |
| $q_{lactate}$ (mmol/gCDW/h) | 0.00386 | 0.00425 | 0.00471 | 0.0043 | 0.0004 | 0.0043 | 0.0004 |
| $q_{succinate}$ (mmol/gCDW/h) | 0.0247 | 0.01715 | 0.01904 | 0.0203 | 0.004 | 0.0222 | 0.004 |
| $q_{CO2}$ (mmol/gCDW/h) | 2.971 | 2.919 | 2.961 | 2.95 | 0.03 | 3.1196 | 0.0158 |
| $q_{O2}$ (mmol/gCDW/h) | −2.867 | −2.846 | −2.855 | −2.86 | 0.011 | −2.8381 | 0.0105 |
| $q_{PHB}$ (mmol/gCDW/h) | 0.0714 | 0.06834 | 0.06507 | 0.0683 | 0.0034 | 0.0676 | 0.0034 |
| $q_{formate}$ (mmol/gCDW/h) | 0.059 | 0.0761 | 0.0662 | 0.0673 | 0.008 | 0.0736 | 0.0079 |

b.d.l.: below detection level.

PAOphaB_XbaDwCrt. Those primers were designed to hybridize with the reference *phaB*$^{CAp}$ (GenBank: Genome CP001715.1, locus_tag="CAP2UW1_3919″) and they added target sequences for the restriction enzymes *BamH*I and *Xba*I in the extremes of the amplified DNA. The PCR product was cleaned (NucleoSpin® Gel and PCR clean-up (Macherey-Nagel)) and restricted with *BamH*I and cloned into the pMiniT vector using a PCR Cloning Kit (New England Biolabs, #E1202). Before perform the ligation into the pMiniT vector, 5′ four base overhangs resulting from restriction with *BamH*I were filled using reagents included in the PCR Cloning Kit. The ligation product was employed to transform NEB-10 beta cells (New England Biolabs, #C3019), included as part of the PCR Cloning Kit. By colony PCR, four colonies bearing plasmids carrying inserts of the expected size were detected. The recombinant plasmids from those clones were isolated and the insertions were amplified using primers provided with the PCR Cloning Kit. The resulting PCR products were sequenced (Baseclear, Netherlands) and the plasmid carrying the insert with the highest identity respect to the annotated *phaB*$^{CAp}$ gene was named pMiniT-phaBCAp. The open reading frame present in pMiniT-phaBCAp was employed for further cloning procedures aiming the recombinant expression of the encoded protein and the construction of an artificial operon together with the *phaCA* genes from *C. necator* (see below).

On the other hand, an artificial DNA sequence, was designed and purchased (IDT, Integrated DNA Technologies, Belgium). This artificial sequence encodes for a version of the acetoacetyl-CoA reductases from *C. necator* (AAR$^{Cn}$) where the original residues N37-S38-P39-R40-R41 were replaced by the residues E37-F38-D39-K40-P41 from AAR$^{CAp}$. This artificial enzyme was named AAR$^{Chimera}$. The amino acid encoding sequences of AAR$^{CAp}$ and AAR$^{Chimera}$ were cloned in the vector pCOLA-duet-1, in frame with a vector DNA sequence encoding for a poly-histidine tail. The relevant DNA sequences of the plasmids pCOLA-His-phaBCAp6 and pCola-phaB-Chimera were checked by sequencing, and these plasmids were introduced in *E. coli* BL21(DE3) cells.

**Table 3**
Metabolic fluxes distributions for the engineered strain during the two studied steady-states. The feasible minimal and maximal fluxes for each reaction is also reported. Metabolites labelled with the symbol [e] are considered extracellular while the symbol [c] signal the intracellular metabolites.

| | | Steady-state 1 | | | Steady-state 2 | | |
|---|---|---|---|---|---|---|---|
| Reaction name | Reaction | Optimal flux (mol/CmolX/h) | Minimum flux (mol/CmolX/h) | Maximum flux (mol/CmolX/h) | Optimal flux (mol/CmolX/h) | Minimum flux (mol/CmolX/h) | Maximum flux (mol/CmolX/h) |
| EX_ac(e) | ac[e] -> | 0.0002 | 0.0002 | 0.0002 | 0.0051 | 0.0051 | 0.0051 |
| EX_acald(e) | acald[e] -> | 0.0000 | 0.0000 | 0.0000 | 0.0000 | 0.0000 | 0.0000 |
| EX_akg(e) | akg[e] -> | 0.0000 | 0.0000 | 0.0000 | 0.0000 | 0.0000 | 0.0000 |
| EX_co2(e) | co2[e] <=> | 0.1028 | 0.1028 | 0.1028 | 0.0721 | 0.0721 | 0.0721 |
| EX_etoh(e) | etoh[e] -> | 0.0000 | 0.0000 | 0.0000 | 0.0000 | 0.0000 | 0.0000 |
| EX_for(e) | for[e] -> | 0.0000 | 0.0000 | 0.0000 | 0.0019 | 0.0019 | 0.0019 |
| EX_fru(e) | fru[e] -> | 0.0000 | 0.0000 | 0.0000 | 0.0000 | 0.0000 | 0.0000 |
| EX_fum(e) | fum[e] -> | 0.0000 | 0.0000 | 0.0000 | 0.0000 | 0.0000 | 0.0000 |
| EX_glc(e) | glc-D[e] -> | 0.0000 | 0.0000 | 0.0000 | 0.0000 | 0.0000 | 0.0000 |
| EX_gln_L(e) | gln-L[e] -> | 0.0000 | 0.0000 | 0.0000 | 0.0000 | 0.0000 | 0.0000 |
| EX_glu_L(e) | glu-L[e] -> | 0.0000 | 0.0000 | 0.0000 | 0.0000 | 0.0000 | 0.0000 |
| EX_h(e) | h[e] <=> | 0.0282 | 0.0282 | 0.0282 | 0.0291 | 0.0291 | 0.0291 |
| EX_h2o(e) | h2o[e] <=> | 0.1442 | 0.1442 | 0.1442 | 0.1082 | 0.1082 | 0.1082 |
| EX_lac_D(e) | lac-D[e] -> | 0.0013 | 0.0013 | 0.0013 | 0.0001 | 0.0001 | 0.0001 |
| EX_mal_L(e) | mal-L[e] -> | 0.0000 | 0.0000 | 0.0000 | 0.0000 | 0.0000 | 0.0000 |
| EX_nh4(e) | nh4[e] <=> | −0.0266 | −0.0266 | −0.0266 | −0.0223 | −0.0223 | −0.0223 |
| EX_o2(e) | o2[e] <=> | −0.0955 | −0.0955 | −0.0955 | −0.0660 | −0.0660 | −0.0660 |
| EX_pi(e) | pi[e] <=> | −0.0007 | −0.0007 | −0.0007 | −0.0006 | −0.0006 | −0.0006 |
| EX_pyr(e) | pyr[e] -> | 0.0000 | 0.0000 | 0.0000 | 0.0000 | 0.0000 | 0.0000 |
| EX_succ(e) | succ[e] -> | 0.0010 | 0.0008 | 0.0010 | 0.0006 | 0.0004 | 0.0006 |
| EX_so4[e] | so4[e] <=> | −0.0007 | −0.0007 | −0.0007 | −0.0006 | −0.0006 | −0.0006 |
| EX_glyc[e] | glyc[e] -> | 0.0000 | 0.0000 | 0.0000 | 0.0000 | 0.0000 | 0.0000 |
| GlucosePTS | glc-D[e] + pep[c] -> g6p[c] + pyr[c] | 0.0000 | 0.0000 | 0.0000 | 0.0000 | 0.0000 | 0.0000 |
| PGI | g6p[c] <=> f6p[c] | 0.0114 | 0.0114 | 0.0114 | 0.0055 | 0.0055 | 0.0055 |
| PFK | f6p[c] + atp[c] -> adp[c] + fdp[c] + h[c] | 0.0313 | 0.0313 | 0.0313 | 0.0249 | 0.0249 | 0.0249 |
| ALD | fdp[c] <=> dhap[c] + g3p[c] | 0.0313 | 0.0313 | 0.0313 | 0.0249 | 0.0249 | 0.0249 |
| TPI | dhap[c] <=> g3p[c] | 0.0301 | 0.0301 | 0.0301 | 0.0239 | 0.0239 | 0.0239 |
| GAPDH | g3p[c] + nad[c] + pi[c] <=> h[c] + 13dpg[c] + nadh[c] | 0.0636 | 0.0636 | 0.0636 | 0.0521 | 0.0521 | 0.0521 |
| PGK | adp[c] + 13dpg[c] <=> atp[c] + 3pg[c] | 0.0636 | 0.0636 | 0.0636 | 0.0521 | 0.0521 | 0.0521 |

(*continued on next page*)

**Table 3** (*continued*)

| Reaction name | Reaction | Steady-state 1 | | | Steady-state 2 | | |
|---|---|---|---|---|---|---|---|
| | | Optimal flux (mol/CmolX/h) | Minimum flux (mol/CmolX/h) | Maximum flux (mol/CmolX/h) | Optimal flux (mol/CmolX/h) | Minimum flux (mol/CmolX/h) | Maximum flux (mol/CmolX/h) |
| PGlycerateM | 3pg[c] <=> 2pg[c] | 0.0575 | 0.0575 | 0.0575 | 0.0469 | 0.0469 | 0.0469 |
| ENO | 2pg[c] <=> pep[c] + h2o[c] | 0.0575 | 0.0575 | 0.0575 | 0.0469 | 0.0469 | 0.0469 |
| PYK | pep[c] + adp[c] + h[c] -> pyr[c] + atp[c] | 0.0468 | 0.0468 | 0.0469 | 0.0383 | 0.0383 | 0.0383 |
| PDH | pyr[c] + nad[c] + coa[c] -> nadh[c] + accoa[c] + co2[c] | 0.0380 | 0.0380 | 0.0380 | 0.0316 | 0.0316 | 0.0316 |
| AKGDH | nad[c] + coa[c] + akg[c] -> nadh[c] + co2[c] + succoa[c] | 0.0273 | 0.0273 | 0.0273 | 0.0147 | 0.0147 | 0.0147 |
| Aconitase | cit[c] <=> icit[c] | 0.0309 | 0.0309 | 0.0309 | 0.0177 | 0.0177 | 0.0177 |
| CS | h2o[c] + accoa[c] + oaa[c] -> h[c] + coa[c] + cit[c] | 0.0309 | 0.0309 | 0.0309 | 0.0177 | 0.0177 | 0.0177 |
| FUM | h2o[c] + fum[c] <=> mal-L[c] | 0.0280 | 0.0280 | 0.0280 | 0.0155 | 0.0155 | 0.0155 |
| ICDH | icit[c] + nadp[c] -> co2[c] + akg[c] + nadph[c] | 0.0309 | 0.0309 | 0.0309 | 0.0177 | 0.0177 | 0.0177 |
| MDH | nad[c] + mal-L[c] <=> h[c] + nadh[c] + oaa[c] | 0.0280 | 0.0280 | 0.0280 | 0.0155 | 0.0155 | 0.0155 |
| SUCDH | fadh[c] + succ[c] -> fum[c] + fadh2[c] | 0.0263 | 0.0263 | 1000 | 0.0141 | 0.0141 | 1000 |
| SCS | adp[c] + pi[c] + succoa[c] -> atp[c] + coa[c] + succ[c] | 0.0259 | 0.0259 | 0.0259 | 0.0135 | 0.0135 | 0.0135 |
| DHFRd | h[c] + nadph[c] + dhf[c] -> nadp[c] + thf[c] | 0.0000 | 0.0000 | 0.0000 | 0.0000 | 0.0000 | 0.0000 |
| PPihydrolase | h2o[c] + ppi[c] -> h[c] + 2 pi[c] | 0.0119 | 0.0119 | 0.0119 | 0.0088 | 0.0088 | 0.0088 |
| PEPC | pep[c] + h2o[c] + co2[c] -> h[c] + pi[c] + oaa[c] | 0.0081 | 0.0081 | 0.0081 | 0.0065 | 0.0065 | 0.0065 |
| G6PDH | g6p[c] + nadp[c] -> h[c] + nadph[c] + 6pgl[c] | 0.0065 | 0.0065 | 0.0065 | 0.0096 | 0.0096 | 0.0096 |
| 6PGlactonase | h2o[c] + 6pgl[c] -> h[c] + 6pgc[c] | 0.0065 | 0.0065 | 0.0065 | 0.0096 | 0.0096 | 0.0096 |
| GND | nadp[c] + 6pgc[c] -> co2[c] + nadph[c] + ru5p-D[c] | 0.0065 | 0.0065 | 0.0065 | 0.0096 | 0.0096 | 0.0096 |
| RibIso | r5p[c] <=> ru5p-D[c] | −0.0045 | −0.0045 | −0.0045 | −0.0051 | −0.0051 | −0.0051 |
| RibEpi | ru5p-D[c] <=> xu5p-D[c] | 0.0020 | 0.0020 | 0.0020 | 0.0044 | 0.0044 | 0.0044 |
| TALA | g3p[c] + s7p[c] <=> f6p[c] + e4p[c] | 0.0016 | 0.0016 | 0.0016 | 0.0027 | 0.0027 | 0.0027 |
| TKT1 | r5p[c] + xu5p-D[c] <=> g3p[c] + s7p[c] | 0.0016 | 0.0016 | 0.0016 | 0.0027 | 0.0027 | 0.0027 |
| TKT2 | xu5p-D[c] + e4p[c] <=> f6p[c] + g3p[c] | 0.0004 | 0.0004 | 0.0004 | 0.0017 | 0.0017 | 0.0017 |
| ATPase | 4 h[e] + adp[c] + pi[c] <=> atp[c] + 3 h[c] + h2o[c] | 0.2528 | 0.2528 | 0.2528 | 0.1769 | 0.1769 | 0.1769 |
| ETC_FADH2 | fadh2[c] + q8[c] -> fadh[c] + q8h2[c] | 0.0263 | 0.0263 | 1000 | 0.0141 | 0.0141 | 1000 |
| ETOH | 2 h[c] + 2 nadh[c] + accoa[c] <=> 2 nad[c] + coa[c] + etoh[c] | 0.0000 | 0.0000 | 0.0000 | 0.0000 | 0.0000 | 0.0000 |
| ACK | adp[c] + actp[c] -> atp[c] + ac[c] | 0.0000 | 0.0000 | 0.0000 | 0.0037 | 0.0037 | 0.0037 |
| LDH | pyr[c] + h[c] + nadh[c] <=> nad[c] + lac-D[c] | 0.0013 | 0.0013 | 0.0013 | 0.0001 | 0.0001 | 0.0001 |
| PTA | pi[c] + accoa[c] <=> coa[c] + actp[c] | 0.0000 | 0.0000 | 0.0000 | 0.0037 | 0.0037 | 0.0037 |
| PGlucoseM | g1p[c] <=> g6p[c] | −0.0001 | −0.0001 | −0.0001 | −0.0001 | −0.0001 | −0.0001 |

(*continued on next page*)

**Table 3** (*continued*)

| Reaction name | Reaction | Steady-state 1 | | | Steady-state 2 | | |
|---|---|---|---|---|---|---|---|
| | | Optimal flux (mol/CmolX/h) | Minimum flux (mol/CmolX/h) | Maximum flux (mol/CmolX/h) | Optimal flux (mol/CmolX/h) | Minimum flux (mol/CmolX/h) | Maximum flux (mol/CmolX/h) |
| CarbonicAnhydrase | h2o[c] + co2[c] <=> h[c] + hco3[c] | 0.0066 | 0.0066 | 0.0066 | 0.0055 | 0.0055 | 0.0055 |
| ATPM | atp[c] + h2o[c] -> adp[c] + h[c] + pi[c] | 0.1572 | 0.0750 | 0.1572 | 0.0919 | 0.0750 | 0.0919 |
| GlycerolKinase | atp[c] + glyc[c] -> adp[c] + h[c] + glyc3p[c] | 0.0000 | 0.0000 | 0.0000 | 0.0000 | 0.0000 | 0.0000 |
| FBPase | fdp[c] + h2o[c] -> f6p[c] + pi[c] | 0.0000 | 0.0000 | 0.0000 | 0.0000 | 0.0000 | 0.0000 |
| PEPCK | atp[c] + oaa[c] -> pep[c] + adp[c] + co2[c] | 0.0000 | 0.0000 | 0.0000 | 0.0000 | 0.0000 | 0.0000 |
| ICL | icit[c] -> succ[c] + glx[c] | 0.0000 | 0.0000 | 0.0000 | 0.0000 | 0.0000 | 0.0000 |
| MALS | h2o[c] + accoa[c] + glx[c] -> h[c] + coa[c] + mal-L[c] | 0.0000 | 0.0000 | 0.0000 | 0.0000 | 0.0000 | 0.0000 |
| pntAB | 2 h[e] + nadh[c] + nadp[c] -> 2 h[c] + nad[c] + nadph[c] | 0.0000 | 0.0000 | 0.0000 | 0.0000 | 0.0000 | 0.0000 |
| UdhA | nad[c] + nadph[c] -> nadh[c] + nadp[c] | 0.0000 | 0.0000 | 0.0000 | 0.0000 | 0.0000 | 0.0000 |
| ED1 | 6pgc[c] -> h2o[c] + KDPG[c] | 0.0000 | 0.0000 | 0.0000 | 0.0000 | 0.0000 | 0.0000 |
| ED2 | KDPG[c] -> pyr[c] + g3p[c] | 0.0000 | 0.0000 | 0.0000 | 0.0000 | 0.0000 | 0.0000 |
| FUMDHq8 | fum[c] + q8h2[c] -> succ[c] + q8[c] | 0.0000 | 0.0000 | 1000.0 | 0.0000 | 0.0000 | 1000 |
| PFL | pyr[c] + coa[c] -> accoa[c] + for[c] | 0.0000 | 0.0000 | 0.0000 | 0.0002 | 0.0002 | 0.0002 |
| Hydrogenase | h[c] + for[c] -> co2[c] + H2[c] | 0.0000 | 0.0000 | 0.0000 | 0.0000 | 0.0000 | 0.0000 |
| EX_H2[c] | H2[c] -> | 0.0000 | 0.0000 | 0.0000 | 0.0000 | 0.0000 | 0.0000 |
| DHAPred | h[c] + dhap[c] + nadh[c] -> nad[c] + glyc3p[c] | 0.0012 | 0.0012 | 0.0012 | 0.0010 | 0.0010 | 0.0010 |
| DHAPred2 | h[c] + dhap[c] + nadph[c] -> nadp[c] + glyc3p[c] | 0.0000 | 0.0000 | 0.0000 | 0.0000 | 0.0000 | 0.0000 |
| r49 | 0.333333 atp[c] + 0.666667 h[c] + 0.333333 h2o[c] + ac[c] -> ac[e] + h[e] + 0.333333 adp[c] + 0.333333 pi[c] | 0.0002 | 0.0002 | 0.0002 | 0.0051 | 0.0051 | 0.0051 |
| r53 | 0.333333 atp[c] + 0.666667 h[c] + 0.333333 h2o[c] + lac-D[c] -> h[e] + lac-D[e] + 0.333333 adp[c] + 0.333333 pi[c] | 0.0013 | 0.0013 | 0.0013 | 0.0001 | 0.0001 | 0.0001 |
| r55 | 0.333333 atp[c] + 0.666667 h[c] + 0.333333 h2o[c] + for[c] -> for[e] + h[e] + 0.333333 adp[c] + 0.333333 pi[c] | 0.0000 | 0.0000 | 0.0000 | 0.0019 | 0.0019 | 0.0019 |
| r60 | 0.333333 atp[c] + 0.666667 h[c] + 0.333333 h2o[c] + succ[c] -> h[e] + succ[e] + 0.333333 adp[c] + 0.333333 pi[c] | 0.0010 | 0.0010 | 0.0010 | 0.0006 | 0.0006 | 0.0006 |
| r51 | co2[c] -> co2[e] | 0.1028 | 0.1028 | 0.1028 | 0.0721 | 0.0721 | 0.0721 |
| r50 | nh4[e] -> nh4[c] | 0.0266 | 0.0266 | 0.0266 | 0.0223 | 0.0223 | 0.0223 |
| r54 | etoh[c] -> etoh[e] | 0.0000 | 0.0000 | 0.0000 | 0.0000 | 0.0000 | 0.0000 |

(*continued on next page*)

**Table 3** (*continued*)

| Reaction name | Reaction | Steady-state 1 | | | Steady-state 2 | | |
|---|---|---|---|---|---|---|---|
| | | Optimal flux (mol/CmolX/h) | Minimum flux (mol/CmolX/h) | Maximum flux (mol/CmolX/h) | Optimal flux (mol/CmolX/h) | Minimum flux (mol/CmolX/h) | Maximum flux (mol/CmolX/h) |
| r11 | atp[c] + h[c] + g1p[c] -> ppi[c] + adpglc[c] | 0.0001 | 0.0001 | 0.0001 | 0.0001 | 0.0001 | 0.0001 |
| r12 | adpglc[c] -> adp[c] + h[c] + glycogen[c] | 0.0001 | 0.0001 | 0.0001 | 0.0001 | 0.0001 | 0.0001 |
| r37 | h[c] + nadph[c] + trdox[c] -> nadp[c] + trdrd[c] | 0.0025 | 0.0025 | 0.0025 | 0.0021 | 0.0021 | 0.0021 |
| r42 | ru5p-D[c] <=> ara5p[c] | 0.0000 | 0.0000 | 0.0000 | 0.0000 | 0.0000 | 0.0000 |
| r43 | 2dr5p[c] -> g3p[c] + acald[c] | 0.0017 | 0.0017 | 0.0017 | 0.0014 | 0.0014 | 0.0014 |
| r46 | r1p[c] <=> r5p[c] | −0.0017 | −0.0017 | −0.0017 | −0.0014 | −0.0014 | −0.0014 |
| r47 | 2dr1p[c] <=> 2dr5p[c] | 0.0017 | 0.0017 | 0.0017 | 0.0014 | 0.0014 | 0.0014 |
| r48 | acald[e] <=> acald[c] | 0.0000 | 0.0000 | 0.0000 | 0.0000 | 0.0000 | 0.0000 |
| r56 | glyc[c] <=> glyc[e] | 0.0000 | 0.0000 | 0.0000 | 0.0000 | 0.0000 | 0.0000 |
| r57 | h2o[e] <=> h2o[c] | −0.1442 | −0.1442 | −0.1442 | −0.1082 | −0.1082 | −0.1082 |
| r58 | o2[e] <=> o2[c] | 0.0955 | 0.0955 | 0.0955 | 0.0660 | 0.0660 | 0.0660 |
| r59 | h[e] + pi[e] <=> h[c] + pi[c] | 0.0007 | 0.0007 | 0.0007 | 0.0006 | 0.0006 | 0.0006 |
| r61 | so4[e] + atp[c] + h2o[c] -> adp[c] + h[c] + pi[c] + so4[c] | 0.0007 | 0.0007 | 0.0007 | 0.0006 | 0.0006 | 0.0006 |
| r62 | ala-L[c] <=> ala-D[c] | 0.0000 | 0.0000 | 0.0000 | 0.0000 | 0.0000 | 0.0000 |
| r63 | atp[c] + nh4[c] + asp-L[c] -> h[c] + ppi[c] + amp[c] + asn-L[c] | 0.0009 | 0.0009 | 0.0009 | 0.0007 | 0.0007 | 0.0007 |
| r64 | akg[c] + asp-L[c] <=> oaa[c] + glu-L[c] | −0.0052 | −0.0052 | −0.0052 | −0.0043 | −0.0043 | −0.0043 |
| r65 | akg[c] + ala-L[c] <=> pyr[c] + glu-L[c] | −0.0019 | −0.0019 | −0.0019 | −0.0016 | −0.0016 | −0.0016 |
| r66 | 3 h2o[c] + dkmpp[c] -> 6 h[c] + pi[c] + for[c] + 2kmb[c] | 0.0000 | 0.0000 | 0.0000 | 0.0000 | 0.0000 | 0.0000 |
| r67 | glu-L[c] + 2kmb[c] -> akg[c] + met-L[c] | 0.0000 | 0.0000 | 0.0000 | 0.0000 | 0.0000 | 0.0000 |
| r68 | 5mdru1p[c] -> h2o[c] + dkmpp[c] | 0.0000 | 0.0000 | 0.0000 | 0.0000 | 0.0000 | 0.0000 |
| r69 | atp[c] + 5mtr[c] -> adp[c] + h[c] + 5mdr1p[c] | 0.0000 | 0.0000 | 0.0000 | 0.0000 | 0.0000 | 0.0000 |
| r70 | 5mdr1p[c] <=> 5mdru1p[c] | 0.0000 | 0.0000 | 0.0000 | 0.0000 | 0.0000 | 0.0000 |
| r71 | atp[c] + acglu[c] -> adp[c] + acg5p[c] | 0.0009 | 0.0009 | 0.0009 | 0.0008 | 0.0008 | 0.0008 |
| r72 | h2o[c] + acorn[c] -> ac[c] + orn[c] | 0.0009 | 0.0009 | 0.0009 | 0.0008 | 0.0008 | 0.0008 |
| r73 | akg[c] + acorn[c] <=> glu-L[c] + acg5sa[c] | −0.0009 | −0.0009 | −0.0009 | −0.0008 | −0.0008 | −0.0008 |
| r74 | h[c] + amet[c] <=> co2[c] + ametam[c] | 0.0000 | 0.0000 | 0.0000 | 0.0000 | 0.0000 | 0.0000 |
| r75 | argsuc[c] <=> fum[c] + arg-L[c] | 0.0008 | 0.0008 | 0.0008 | 0.0007 | 0.0007 | 0.0007 |
| r76 | atp[c] + asp-L[c] + citr-L[c] -> h[c] + ppi[c] + amp[c] + argsuc[c] | 0.0008 | 0.0008 | 0.0008 | 0.0007 | 0.0007 | 0.0007 |
| r77 | 2 atp[c] + h2o[c] + hco3[c] + gln-L[c] -> 2 adp[c] + 2 h[c] + pi[c] + glu-L[c] + cbp[c] | 0.0011 | 0.0011 | 0.0011 | 0.0009 | 0.0009 | 0.0009 |

(*continued on next page*)

**Table 3** (*continued*)

| Reaction name | Reaction | Steady-state 1 | | | Steady-state 2 | | |
|---|---|---|---|---|---|---|---|
| | | Optimal flux (mol/CmolX/h) | Minimum flux (mol/CmolX/h) | Maximum flux (mol/CmolX/h) | Optimal flux (mol/CmolX/h) | Minimum flux (mol/CmolX/h) | Maximum flux (mol/CmolX/h) |
| r78 | atp[c] + glu-L[c] -> adp[c] + glu5p[c] | 0.0007 | 0.0007 | 0.0007 | 0.0006 | 0.0006 | 0.0006 |
| r79 | h[c] + nadph[c] + glu5p[c] -> pi[c] + nadp[c] + glu5sa[c] | 0.0007 | 0.0007 | 0.0007 | 0.0006 | 0.0006 | 0.0006 |
| r80 | glu5sa[c] -> h[c] + h2o[c] + 1pyr5c[c] | 0.0007 | 0.0007 | 0.0007 | 0.0006 | 0.0006 | 0.0006 |
| r81 | h2o[c] + 5mta[c] -> 5mtr[c] + ade[c] | 0.0000 | 0.0000 | 0.0000 | 0.0000 | 0.0000 | 0.0000 |
| r82 | pi[c] + nadp[c] + acg5sa[c] <=> h[c] + nadph[c] + acg5p[c] | −0.0009 | −0.0009 | −0.0009 | −0.0008 | −0.0008 | −0.0008 |
| r83 | accoa[c] + glu-L[c] -> h[c] + coa[c] + acglu[c] | 0.0009 | 0.0009 | 0.0009 | 0.0008 | 0.0008 | 0.0008 |
| r84 | orn[c] + cbp[c] <=> h[c] + pi[c] + citr-L[c] | 0.0008 | 0.0008 | 0.0008 | 0.0007 | 0.0007 | 0.0007 |
| r85 | h[c] + orn[c] -> co2[c] + ptrc[c] | 0.0001 | 0.0001 | 0.0001 | 0.0001 | 0.0001 | 0.0001 |
| r86 | 2 h[c] + nadph[c] + 1pyr5c[c] -> nadp[c] + pro-L[c] | 0.0007 | 0.0007 | 0.0007 | 0.0006 | 0.0006 | 0.0006 |
| r87 | ametam[c] + ptrc[c] -> h[c] + 5mta[c] + spmd[c] | 0.0000 | 0.0000 | 0.0000 | 0.0000 | 0.0000 | 0.0000 |
| r88 | h2o[c] + pap[c] -> pi[c] + amp[c] | 0.0007 | 0.0007 | 0.0007 | 0.0006 | 0.0006 | 0.0006 |
| r89 | atp[c] + aps[c] -> adp[c] + h[c] + paps[c] | 0.0007 | 0.0007 | 0.0007 | 0.0006 | 0.0006 | 0.0006 |
| r90 | acser[c] + h2s[c] -> h[c] + ac[c] + cys-L[c] | 0.0007 | 0.0007 | 0.0007 | 0.0006 | 0.0006 | 0.0006 |
| r91 | trdrd[c] + paps[c] -> 2 h[c] + trdox[c] + pap[c] + so3[c] | 0.0007 | 0.0007 | 0.0007 | 0.0006 | 0.0006 | 0.0006 |
| r92 | accoa[c] + ser-L[c] <=> coa[c] + acser[c] | 0.0007 | 0.0007 | 0.0007 | 0.0006 | 0.0006 | 0.0006 |
| r93 | atp[c] + h2o[c] + so4[c] + gtp[c] -> pi[c] + ppi[c] + aps[c] + gdp[c] | 0.0007 | 0.0007 | 0.0007 | 0.0006 | 0.0006 | 0.0006 |
| r94 | 5 h[c] + 3 nadph[c] + so3[c] -> 3 h2o[c] + 3 nadp[c] + h2s[c] | 0.0007 | 0.0007 | 0.0007 | 0.0006 | 0.0006 | 0.0006 |
| r95 | h[c] + akg[c] + nadph[c] + nh4[c] -> h2o[c] + nadp[c] + glu-L[c] | 0.0231 | 0.0231 | 0.0231 | 0.0194 | 0.0194 | 0.0194 |
| r96 | atp[c] + nh4[c] + glu-L[c] -> adp[c] + h[c] + pi[c] + gln-L[c] | 0.0037 | 0.0037 | 0.0037 | 0.0031 | 0.0031 | 0.0031 |
| r97 | thf[c] + ser-L[c] -> h2o[c] + gly[c] + mlthf[c] | 0.0035 | 0.0035 | 0.0035 | 0.0029 | 0.0029 | 0.0029 |
| r98 | nad[c] + 3pg[c] -> h[c] + nadh[c] + 3php[c] | 0.0061 | 0.0061 | 0.0061 | 0.0052 | 0.0052 | 0.0052 |
| r99 | h2o[c] + pser-L[c] -> pi[c] + ser-L[c] | 0.0061 | 0.0061 | 0.0061 | 0.0052 | 0.0052 | 0.0052 |
| r100 | glu-L[c] + 3php[c] -> akg[c] + pser-L[c] | 0.0061 | 0.0061 | 0.0061 | 0.0052 | 0.0052 | 0.0052 |
| r101 | prfp[c] -> prlp[c] | 0.0003 | 0.0003 | 0.0003 | 0.0003 | 0.0003 | 0.0003 |
| r102 | atp[c] + prpp[c] -> ppi[c] + prbatp[c] | 0.0003 | 0.0003 | 0.0003 | 0.0003 | 0.0003 | 0.0003 |
| r103 | 2 nad[c] + h2o[c] + histd[c] -> 3 h[c] + 2 nadh[c] + his-L[c] | 0.0003 | 0.0003 | 0.0003 | 0.0003 | 0.0003 | 0.0003 |
| r104 | h2o[c] + hisp[c] -> pi[c] + histd[c] | 0.0003 | 0.0003 | 0.0003 | 0.0003 | 0.0003 | 0.0003 |
| r105 | glu-L[c] + imacp[c] -> akg[c] + hisp[c] | 0.0003 | 0.0003 | 0.0003 | 0.0003 | 0.0003 | 0.0003 |
| r106 | gln-L[c] + prlp[c] -> h[c] + glu-L[c] + aicar[c] + eig3p[c] | 0.0003 | 0.0003 | 0.0003 | 0.0003 | 0.0003 | 0.0003 |
| r107 | eig3p[c] -> h2o[c] + imacp[c] | 0.0003 | 0.0003 | 0.0003 | 0.0003 | 0.0003 | 0.0003 |

(*continued on next page*)

**Table 3** (*continued*)

| Reaction name | Reaction | Steady-state 1 | | | Steady-state 2 | | |
|---|---|---|---|---|---|---|---|
| | | Optimal flux (mol/CmolX/h) | Minimum flux (mol/CmolX/h) | Maximum flux (mol/CmolX/h) | Optimal flux (mol/CmolX/h) | Minimum flux (mol/CmolX/h) | Maximum flux (mol/CmolX/h) |
| r108 | h2o[c] + prbamp[c] -> prfp[c] | 0.0003 | 0.0003 | 0.0003 | 0.0003 | 0.0003 | 0.0003 |
| r109 | h2o[c] + prbatp[c] -> h[c] + ppi[c] + prbamp[c] | 0.0003 | 0.0003 | 0.0003 | 0.0003 | 0.0003 | 0.0003 |
| r110 | atp[c] + r5p[c] <=> h[c] + amp[c] + prpp[c] | 0.0011 | 0.0011 | 0.0011 | 0.0010 | 0.0010 | 0.0010 |
| r111 | h2o[c] + cyst-L[c] -> pyr[c] + nh4[c] + hcys-L[c] | 0.0004 | 0.0004 | 0.0004 | 0.0004 | 0.0004 | 0.0004 |
| r112 | succoa[c] + hom-L[c] -> coa[c] + suchms[c] | 0.0004 | 0.0004 | 0.0004 | 0.0004 | 0.0004 | 0.0004 |
| r113 | atp[c] + h2o[c] + met-L[c] -> pi[c] + ppi[c] + amet[c] | 0.0000 | 0.0000 | 0.0000 | 0.0000 | 0.0000 | 0.0000 |
| r114 | hcys-L[c] + 5mthf[c] -> thf[c] + met-L[c] | 0.0004 | 0.0004 | 0.0004 | 0.0004 | 0.0004 | 0.0004 |
| r115 | cys-L[c] + suchms[c] -> h[c] + succ[c] + cyst-L[c] | 0.0004 | 0.0004 | 0.0004 | 0.0004 | 0.0004 | 0.0004 |
| r116 | atp[c] + asp-L[c] <=> adp[c] + 4pasp[c] | 0.0014 | 0.0014 | 0.0014 | 0.0012 | 0.0012 | 0.0012 |
| r117 | pi[c] + nadp[c] + aspsa[c] <=> h[c] + nadph[c] + 4pasp[c] | −0.0014 | −0.0014 | −0.0014 | −0.0012 | −0.0012 | −0.0012 |
| r118 | h[c] + 26dap-M[c] -> co2[c] + lys-L[c] | 0.0010 | 0.0010 | 0.0010 | 0.0008 | 0.0008 | 0.0008 |
| r119 | 26dap-LL[c] <=> 26dap-M[c] | 0.0010 | 0.0010 | 0.0010 | 0.0008 | 0.0008 | 0.0008 |
| r120 | h[c] + nadph[c] + 23dhdp[c] -> nadp[c] + thdp[c] | 0.0010 | 0.0010 | 0.0010 | 0.0008 | 0.0008 | 0.0008 |
| r121 | pyr[c] + aspsa[c] -> h[c] + 2 h2o[c] + 23dhdp[c] | 0.0010 | 0.0010 | 0.0010 | 0.0008 | 0.0008 | 0.0008 |
| r122 | nadp[c] + hom-L[c] <=> h[c] + nadph[c] + aspsa[c] | −0.0004 | −0.0004 | −0.0004 | −0.0004 | −0.0004 | −0.0004 |
| r123 | h2o[c] + sl26da[c] -> succ[c] + 26dap-LL[c] | 0.0010 | 0.0010 | 0.0010 | 0.0008 | 0.0008 | 0.0008 |
| r124 | akg[c] + sl26da[c] <=> glu-L[c] + sl2a6o[c] | −0.0010 | −0.0010 | −0.0010 | −0.0008 | −0.0008 | −0.0008 |
| r125 | h2o[c] + succoa[c] + thdp[c] -> coa[c] + sl2a6o[c] | 0.0010 | 0.0010 | 0.0010 | 0.0008 | 0.0008 | 0.0008 |
| r126 | thr-L[c] <=> acald[c] + gly[c] | −0.0017 | −0.0017 | −0.0017 | −0.0014 | −0.0014 | −0.0014 |
| r127 | 3dhq[c] <=> h2o[c] + 3dhsk[c] | 0.0012 | 0.0012 | 0.0012 | 0.0010 | 0.0010 | 0.0010 |
| r128 | 2dda7p[c] -> pi[c] + 3dhq[c] | 0.0012 | 0.0012 | 0.0012 | 0.0010 | 0.0010 | 0.0010 |
| r129 | pep[c] + h2o[c] + e4p[c] -> pi[c] + 2dda7p[c] | 0.0012 | 0.0012 | 0.0012 | 0.0010 | 0.0010 | 0.0010 |
| r130 | pep[c] + skm5p[c] <=> pi[c] + 3psme[c] | 0.0012 | 0.0012 | 0.0012 | 0.0010 | 0.0010 | 0.0010 |
| r131 | prpp[c] + anth[c] -> ppi[c] + pran[c] | 0.0002 | 0.0002 | 0.0002 | 0.0002 | 0.0002 | 0.0002 |
| r132 | gln-L[c] + chor[c] -> pyr[c] + h[c] + glu-L[c] + anth[c] | 0.0002 | 0.0002 | 0.0002 | 0.0002 | 0.0002 | 0.0002 |
| r133 | chor[c] -> pphn[c] | 0.0011 | 0.0011 | 0.0011 | 0.0009 | 0.0009 | 0.0009 |
| r134 | 3psme[c] -> pi[c] + chor[c] | 0.0012 | 0.0012 | 0.0012 | 0.0010 | 0.0010 | 0.0010 |
| r135 | h[c] + 2cpr5p[c] -> h2o[c] + co2[c] + 3ig3p[c] | 0.0002 | 0.0002 | 0.0002 | 0.0002 | 0.0002 | 0.0002 |
| r136 | akg[c] + phe-L[c] <=> glu-L[c] + phpyr[c] | −0.0006 | −0.0006 | −0.0006 | −0.0005 | −0.0005 | −0.0005 |
| r137 | pran[c] -> 2cpr5p[c] | 0.0002 | 0.0002 | 0.0002 | 0.0002 | 0.0002 | 0.0002 |
| r138 | h[c] + pphn[c] -> h2o[c] + co2[c] + phpyr[c] | 0.0006 | 0.0006 | 0.0006 | 0.0005 | 0.0005 | 0.0005 |

(*continued on next page*)

**Table 3** (*continued*)

| Reaction name | Reaction | Steady-state 1 | | | Steady-state 2 | | |
|---|---|---|---|---|---|---|---|
| | | Optimal flux (mol/CmolX/h) | Minimum flux (mol/CmolX/h) | Maximum flux (mol/CmolX/h) | Optimal flux (mol/CmolX/h) | Minimum flux (mol/CmolX/h) | Maximum flux (mol/CmolX/h) |
| r139 | nad[c] + pphn[c] -> nadh[c] + co2[c] + 34hpp[c] | 0.0005 | 0.0005 | 0.0005 | 0.0004 | 0.0004 | 0.0004 |
| r140 | h[c] + nadph[c] + 3dhsk[c] <=> nadp[c] + skm[c] | 0.0012 | 0.0012 | 0.0012 | 0.0010 | 0.0010 | 0.0010 |
| r141 | atp[c] + skm[c] -> adp[c] + h[c] + skm5p[c] | 0.0012 | 0.0012 | 0.0012 | 0.0010 | 0.0010 | 0.0010 |
| r142 | 3ig3p[c] -> g3p[c] + indole[c] | 0.0002 | 0.0002 | 0.0002 | 0.0002 | 0.0002 | 0.0002 |
| r143 | h2o[c] + trp-L[c] <=> pyr[c] + nh4[c] + indole[c] | −0.0002 | −0.0002 | −0.0002 | −0.0002 | −0.0002 | −0.0002 |
| r144 | akg[c] + tyr-L[c] <=> glu-L[c] + 34hpp[c] | −0.0005 | −0.0005 | −0.0005 | −0.0004 | −0.0004 | −0.0004 |
| r145 | pyr[c] + h[c] + 2obut[c] -> co2[c] + 2ahbut[c] | 0.0008 | 0.0008 | 0.0008 | 0.0007 | 0.0007 | 0.0007 |
| r146 | h2o[c] + 2ippm[c] <=> 3c3hmp[c] | −0.0009 | −0.0009 | −0.0009 | −0.0007 | −0.0007 | −0.0007 |
| r147 | h2o[c] + accoa[c] + 3mob[c] -> h[c] + coa[c] + 3c3hmp[c] | 0.0009 | 0.0009 | 0.0009 | 0.0007 | 0.0007 | 0.0007 |
| r148 | h[c] + 3c4mop[c] -> co2[c] + 4mop[c] | 0.0009 | 0.0009 | 0.0009 | 0.0007 | 0.0007 | 0.0007 |
| r149 | 3c2hmp[c] <=> h2o[c] + 2ippm[c] | −0.0009 | −0.0009 | −0.0009 | −0.0007 | −0.0007 | −0.0007 |
| r150 | nad[c] + 3c2hmp[c] -> h[c] + nadh[c] + 3c4mop[c] | 0.0009 | 0.0009 | 0.0009 | 0.0007 | 0.0007 | 0.0007 |
| r151 | h[c] + nadph[c] + alac-S[c] -> nadp[c] + 23dhmb[c] | 0.0021 | 0.0021 | 0.0021 | 0.0018 | 0.0018 | 0.0018 |
| r152 | 2 pyr[c] + h[c] -> co2[c] + alac-S[c] | 0.0021 | 0.0021 | 0.0021 | 0.0018 | 0.0018 | 0.0018 |
| r153 | 23dhmb[c] -> h2o[c] + 3mob[c] | 0.0021 | 0.0021 | 0.0021 | 0.0018 | 0.0018 | 0.0018 |
| r154 | 23dhmp[c] -> h2o[c] + 3mop[c] | 0.0008 | 0.0008 | 0.0008 | 0.0007 | 0.0007 | 0.0007 |
| r155 | akg[c] + ile-L[c] <=> glu-L[c] + 3mop[c] | −0.0008 | −0.0008 | −0.0008 | −0.0007 | −0.0007 | −0.0007 |
| r156 | h[c] + nadph[c] + 2ahbut[c] -> nadp[c] + 23dhmp[c] | 0.0008 | 0.0008 | 0.0008 | 0.0007 | 0.0007 | 0.0007 |
| r157 | glu-L[c] + 4mop[c] -> akg[c] + leu-L[c] | 0.0009 | 0.0009 | 0.0009 | 0.0007 | 0.0007 | 0.0007 |
| r158 | thr-L[c] -> nh4[c] + 2obut[c] | 0.0008 | 0.0008 | 0.0008 | 0.0007 | 0.0007 | 0.0007 |
| r159 | akg[c] + val-L[c] <=> glu-L[c] + 3mob[c] | −0.0012 | −0.0012 | −0.0012 | −0.0010 | −0.0010 | −0.0010 |
| r160 | pep[c] + h2o[c] + ara5p[c] -> pi[c] + kdo8p[c] | 0.0000 | 0.0000 | 0.0000 | 0.0000 | 0.0000 | 0.0000 |
| r161 | ckdo[c] + lipidA[c] -> h[c] + cmp[c] + kdolipid4[c] | 0.0000 | 0.0000 | 0.0000 | 0.0000 | 0.0000 | 0.0000 |
| r162 | ckdo[c] + kdolipid4[c] -> h[c] + cmp[c] + kdo2lipid4[c] | 0.0000 | 0.0000 | 0.0000 | 0.0000 | 0.0000 | 0.0000 |
| r163 | ctp[c] + kdo[c] -> ppi[c] + ckdo[c] | 0.0000 | 0.0000 | 0.0000 | 0.0000 | 0.0000 | 0.0000 |
| r164 | h2o[c] + kdo8p[c] -> pi[c] + kdo[c] | 0.0000 | 0.0000 | 0.0000 | 0.0000 | 0.0000 | 0.0000 |
| r165 | atp[c] + ACP[c] + ttdcea[c] -> ppi[c] + amp[c] + tdeACP[c] | 0.0002 | 0.0002 | 0.0002 | 0.0002 | 0.0002 | 0.0002 |
| r166 | atp[c] + ACP[c] + hdca[c] -> ppi[c] + amp[c] + palmACP[c] | 0.0013 | 0.0013 | 0.0013 | 0.0011 | 0.0011 | 0.0011 |
| r167 | atp[c] + ACP[c] + hdcea[c] -> ppi[c] + amp[c] + hdeACP[c] | 0.0001 | 0.0001 | 0.0001 | 0.0001 | 0.0001 | 0.0001 |
| r168 | atp[c] + ACP[c] + ocdcea[c] -> ppi[c] + amp[c] + octeACP[c] | 0.0021 | 0.0021 | 0.0021 | 0.0018 | 0.0018 | 0.0018 |
| r169 | atp[c] + ACP[c] + ttdca[c] -> ppi[c] + amp[c] + myrsACP[c] | 0.0001 | 0.0001 | 0.0001 | 0.0001 | 0.0001 | 0.0001 |
| r170 | adphep-D,D[c] -> adphep-L,D[c] | 0.0000 | 0.0000 | 0.0000 | 0.0000 | 0.0000 | 0.0000 |

(*continued on next page*)

**Table 3** (*continued*)

| Reaction name | Reaction | Steady-state 1 | | | Steady-state 2 | | |
|---|---|---|---|---|---|---|---|
| | | Optimal flux (mol/CmolX/h) | Minimum flux (mol/CmolX/h) | Maximum flux (mol/CmolX/h) | Optimal flux (mol/CmolX/h) | Minimum flux (mol/CmolX/h) | Maximum flux (mol/CmolX/h) |
| r171 | atp[c] + 2 ala-D[c] <=> adp[c] + h[c] + pi[c] + alaala[c] | 0.0000 | 0.0000 | 0.0000 | 0.0000 | 0.0000 | 0.0000 |
| r172 | atp[c] + h[c] + gmhep1p[c] -> ppi[c] + adphep-D,D[c] | 0.0000 | 0.0000 | 0.0000 | 0.0000 | 0.0000 | 0.0000 |
| r173 | h2o[c] + gmhep17bp[c] -> pi[c] + gmhep1p[c] | 0.0000 | 0.0000 | 0.0000 | 0.0000 | 0.0000 | 0.0000 |
| r174 | atp[c] + gmhep7p[c] -> adp[c] + h[c] + gmhep17bp[c] | 0.0000 | 0.0000 | 0.0000 | 0.0000 | 0.0000 | 0.0000 |
| r175 | atp[c] + 0.02 12dgr_EC[c] -> adp[c] + h[c] + 0.02 pa_EC[c] | 0.0000 | 0.0000 | 0.0000 | 0.0000 | 0.0000 | 0.0000 |
| r176 | kdo2lipid4[c] + ddcaACP[c] -> ACP[c] + kdo2lipid4L[c] | 0.0000 | 0.0000 | 0.0000 | 0.0000 | 0.0000 | 0.0000 |
| r177 | myrsACP[c] + kdo2lipid4L[c] -> ACP[c] + lipa[c] | 0.0000 | 0.0000 | 0.0000 | 0.0000 | 0.0000 | 0.0000 |
| r178 | h[c] + cmp[c] + 0.02 pe_EC[c] <=> 0.02 12dgr_EC[c] + cdpea[c] | 0.0000 | 0.0000 | 0.0000 | 0.0000 | 0.0000 | 0.0000 |
| r179 | accoa[c] + gam1p[c] -> h[c] + coa[c] + acgam1p[c] | 0.0000 | 0.0000 | 0.0000 | 0.0000 | 0.0000 | 0.0000 |
| r180 | glu-D[c] <=> glu-L[c] | 0.0000 | 0.0000 | 0.0000 | 0.0000 | 0.0000 | 0.0000 |
| r181 | f6p[c] + gln-L[c] -> glu-L[c] + gam6p[c] | 0.0000 | 0.0000 | 0.0000 | 0.0000 | 0.0000 | 0.0000 |
| r182 | h2o[c] + g3pe[c] -> h[c] + glyc3p[c] + etha[c] | 0.0011 | 0.0011 | 0.0011 | 0.0009 | 0.0009 | 0.0009 |
| r183 | h2o[c] + g3pg[c] -> h[c] + glyc[c] + glyc3p[c] | 0.0012 | 0.0012 | 0.0012 | 0.0010 | 0.0010 | 0.0010 |
| r184 | lipidX[c] + u23ga[c] -> h[c] + lipidAds[c] + udp[c] | 0.0000 | 0.0000 | 0.0000 | 0.0000 | 0.0000 | 0.0000 |
| r185 | 3 ckdo[c] + 3 adphep-L,D[c] + lipa[c] + 2 cdpea[c] + 2 udpg[c] -> 3 adp[c] + 10 h[c] + 3 cmp[c] + 2 udp[c] + 2 cdp[c] + lps_EC[c] | 0.0000 | 0.0000 | 0.0000 | 0.0000 | 0.0000 | 0.0000 |
| r186 | h2o[c] + 0.02 agpe_EC[c] -> h[c] + 0.05 ttdcea[c] + 0.36 hdca[c] + 0.07 hdcea[c] + 0.5 ocdcea[c] + 0.02 ttdca[c] + g3pe[c] | 0.0011 | 0.0011 | 0.0011 | 0.0009 | 0.0009 | 0.0009 |
| r187 | h2o[c] + 0.02 agpg_EC[c] -> h[c] + 0.05 ttdcea[c] + 0.36 hdca[c] + 0.07 hdcea[c] + 0.5 ocdcea[c] + 0.02 ttdca[c] + g3pg[c] | 0.0012 | 0.0012 | 0.0012 | 0.0010 | 0.0010 | 0.0010 |
| r188 | uaagmda[c] -> h[c] + peptido_EC[c] + udcpdp[c] | 0.0000 | 0.0000 | 0.0000 | 0.0000 | 0.0000 | 0.0000 |
| r189 | h2o[c] + 0.02 pe_EC[c] -> h[c] + 0.05 ttdcea[c] + 0.36 hdca[c] + 0.07 hdcea[c] + 0.5 ocdcea[c] + 0.02 ttdca[c] + 0.02 agpe_EC[c] | 0.0011 | 0.0011 | 0.0011 | 0.0009 | 0.0009 | 0.0009 |
| r190 | gam1p[c] <=> gam6p[c] | 0.0000 | 0.0000 | 0.0000 | 0.0000 | 0.0000 | 0.0000 |
| r191 | h2o[c] + 0.02 pg_EC[c] -> h[c] + 0.05 ttdcea[c] + 0.36 hdca[c] + 0.07 hdcea[c] + 0.5 ocdcea[c] + 0.02 ttdca[c] + 0.02 agpg_EC[c] | 0.0012 | 0.0012 | 0.0012 | 0.0010 | 0.0010 | 0.0010 |
| r192 | udcpp[c] + ugmda[c] -> uagmda[c] + ump[c] | 0.0000 | 0.0000 | 0.0000 | 0.0000 | 0.0000 | 0.0000 |
| r193 | s7p[c] -> gmhep7p[c] | 0.0000 | 0.0000 | 0.0000 | 0.0000 | 0.0000 | 0.0000 |

(*continued on next page*)

**Table 3** (*continued*)

| Reaction name | Reaction | Steady-state 1 | | | Steady-state 2 | | |
|---|---|---|---|---|---|---|---|
| | | Optimal flux (mol/CmolX/h) | Minimum flux (mol/CmolX/h) | Maximum flux (mol/CmolX/h) | Optimal flux (mol/CmolX/h) | Minimum flux (mol/CmolX/h) | Maximum flux (mol/CmolX/h) |
| r194 | atp[c] + lipidAds[c] -> adp[c] + h[c] + lipidA[c] | 0.0000 | 0.0000 | 0.0000 | 0.0000 | 0.0000 | 0.0000 |
| r195 | 3hmrsACP[c] + u3hga[c] -> h[c] + ACP[c] + u23ga[c] | 0.0000 | 0.0000 | 0.0000 | 0.0000 | 0.0000 | 0.0000 |
| r196 | h2o[c] + u3aga[c] -> ac[c] + u3hga[c] | 0.0000 | 0.0000 | 0.0000 | 0.0000 | 0.0000 | 0.0000 |
| r197 | h[c] + nadph[c] + uaccg[c] -> nadp[c] + uamr[c] | 0.0000 | 0.0000 | 0.0000 | 0.0000 | 0.0000 | 0.0000 |
| r198 | pep[c] + uacgam[c] -> pi[c] + uaccg[c] | 0.0000 | 0.0000 | 0.0000 | 0.0000 | 0.0000 | 0.0000 |
| r199 | 3hmrsACP[c] + uacgam[c] <=> ACP[c] + u3aga[c] | 0.0000 | 0.0000 | 0.0000 | 0.0000 | 0.0000 | 0.0000 |
| r200 | h[c] + acgam1p[c] + utp[c] -> ppi[c] + uacgam[c] | 0.0000 | 0.0000 | 0.0000 | 0.0000 | 0.0000 | 0.0000 |
| r201 | uagmda[c] + uacgam[c] -> h[c] + udp[c] + uaagmda[c] | 0.0000 | 0.0000 | 0.0000 | 0.0000 | 0.0000 | 0.0000 |
| r202 | atp[c] + ala-L[c] + uamr[c] -> adp[c] + h[c] + pi[c] + uama[c] | 0.0000 | 0.0000 | 0.0000 | 0.0000 | 0.0000 | 0.0000 |
| r203 | atp[c] + glu-D[c] + uama[c] -> adp[c] + h[c] + pi[c] + uamag[c] | 0.0000 | 0.0000 | 0.0000 | 0.0000 | 0.0000 | 0.0000 |
| r204 | atp[c] + 26dap-M[c] + uamag[c] -> adp[c] + h[c] + pi[c] + ugmd[c] | 0.0000 | 0.0000 | 0.0000 | 0.0000 | 0.0000 | 0.0000 |
| r205 | atp[c] + alaala[c] + ugmd[c] -> adp[c] + h[c] + pi[c] + ugmda[c] | 0.0000 | 0.0000 | 0.0000 | 0.0000 | 0.0000 | 0.0000 |
| r206 | h2o[c] + u23ga[c] -> 2 h[c] + lipidX[c] + ump[c] | 0.0000 | 0.0000 | 0.0000 | 0.0000 | 0.0000 | 0.0000 |
| r207 | h2o[c] + udcpdp[c] -> h[c] + pi[c] + udcpp[c] | 0.0000 | 0.0000 | 0.0000 | 0.0000 | 0.0000 | 0.0000 |
| r208 | h[c] + g1p[c] + utp[c] <=> ppi[c] + udpg[c] | 0.0000 | 0.0000 | 0.0000 | 0.0000 | 0.0000 | 0.0000 |
| r209 | h[c] + nadh[c] + mlthf[c] -> nad[c] + 5mthf[c] | 0.0004 | 0.0004 | 0.0004 | 0.0004 | 0.0004 | 0.0004 |
| r210 | h2o[c] + 10fthf[c] -> h[c] + thf[c] + for[c] | 0.0020 | 0.0020 | 0.0020 | 0.0017 | 0.0017 | 0.0017 |
| r211 | h2o[c] + methf[c] <=> 10fthf[c] | 0.0031 | 0.0031 | 0.0031 | 0.0026 | 0.0026 | 0.0026 |
| r212 | nadp[c] + mlthf[c] <=> h[c] + nadph[c] + methf[c] | 0.0031 | 0.0031 | 0.0031 | 0.0026 | 0.0026 | 0.0026 |
| r213 | 2 h[c] + nadph[c] + ddcaACP[c] + malACP[c] -> co2[c] + nadp[c] + ACP[c] + 3hmrsACP[c] | 0.0000 | 0.0000 | 0.0000 | 0.0000 | 0.0000 | 0.0000 |
| r214 | atp[c] + accoa[c] + hco3[c] <=> adp[c] + h[c] + pi[c] + malcoa[c] | 0.0051 | 0.0051 | 0.0051 | 0.0043 | 0.0043 | 0.0043 |
| r215 | h[c] + accoa[c] + malACP[c] -> coa[c] + co2[c] + actACP[c] | 0.0007 | 0.0007 | 0.0007 | 0.0006 | 0.0006 | 0.0006 |
| r216 | h[c] + ctp[c] + 0.02 pa_EC[c] <=> ppi[c] + 0.02 cdpdag1[c] | 0.0023 | 0.0023 | 0.0023 | 0.0019 | 0.0019 | 0.0019 |
| r217 | 14 h[c] + 10 nadph[c] + 4 malACP[c] + actACP[c] -> 5 h2o[c] + 4 co2[c] + 10 nadp[c] + 4 ACP[c] + ddcaACP[c] | 0.0000 | 0.0000 | 0.0000 | 0.0000 | 0.0000 | 0.0000 |
| r218 | 17 h[c] + 12 nadph[c] + 5 malACP[c] + actACP[c] -> 6 h2o[c] + 5 co2[c] + 12 nadp[c] + 5 ACP[c] + myrsACP[c] | 0.0000 | 0.0000 | 0.0000 | 0.0000 | 0.0000 | 0.0000 |

(*continued on next page*)

**Table 3** (*continued*)

| Reaction name | Reaction | Steady-state 1 | | | Steady-state 2 | | |
|---|---|---|---|---|---|---|---|
| | | Optimal flux (mol/CmolX/h) | Minimum flux (mol/CmolX/h) | Maximum flux (mol/CmolX/h) | Optimal flux (mol/CmolX/h) | Minimum flux (mol/CmolX/h) | Maximum flux (mol/CmolX/h) |
| r219 | 20 h[c] + 14 nadph[c] + 6 malACP[c] + actACP[c] -> 7 h2o[c] + 6 co2[c] + 14 nadp[c] + 6 ACP[c] + palmACP[c] | 0.0003 | 0.0003 | 0.0003 | 0.0003 | 0.0003 | 0.0003 |
| r220 | 19 h[c] + 13 nadph[c] + 6 malACP[c] + actACP[c] -> 7 h2o[c] + 6 co2[c] + 13 nadp[c] + 6 ACP[c] + hdeACP[c] | 0.0002 | 0.0002 | 0.0002 | 0.0002 | 0.0002 | 0.0002 |
| r221 | 22 h[c] + 15 nadph[c] + 7 malACP[c] + actACP[c] -> 8 h2o[c] + 7 co2[c] + 15 nadp[c] + 7 ACP[c] + octeACP[c] | 0.0002 | 0.0002 | 0.0002 | 0.0001 | 0.0001 | 0.0001 |
| r222 | ACP[c] + malcoa[c] <=> coa[c] + malACP[c] | 0.0051 | 0.0051 | 0.0051 | 0.0043 | 0.0043 | 0.0043 |
| r223 | glyc3p[c] + 0.1 tdeACP[c] + 0.72 palmACP[c] + 0.14 hdeACP[c] + octeACP[c] + 0.04 myrsACP[c] -> 2 ACP[c] + 0.02 pa_EC[c] | 0.0023 | 0.0023 | 0.0023 | 0.0019 | 0.0019 | 0.0019 |
| r224 | h2o[c] + 0.02 pgp_EC[c] -> pi[c] + 0.02 pg_EC[c] | 0.0012 | 0.0012 | 0.0012 | 0.0010 | 0.0010 | 0.0010 |
| r225 | glyc3p[c] + 0.02 cdpdag1[c] <=> h[c] + cmp[c] + 0.02 pgp_EC[c] | 0.0012 | 0.0012 | 0.0012 | 0.0010 | 0.0010 | 0.0010 |
| r226 | h[c] + 0.02 ps_EC[c] -> co2[c] + 0.02 pe_EC[c] | 0.0011 | 0.0011 | 0.0011 | 0.0009 | 0.0009 | 0.0009 |
| r227 | ser-L[c] + 0.02 cdpdag1[c] <=> h[c] + cmp[c] + 0.02 ps_EC[c] | 0.0011 | 0.0011 | 0.0011 | 0.0009 | 0.0009 | 0.0009 |
| r228 | h2o[c] + damp[c] -> pi[c] + dad-2[c] | 0.0017 | 0.0017 | 0.0017 | 0.0014 | 0.0014 | 0.0014 |
| r229 | atp[c] + adn[c] -> adp[c] + h[c] + amp[c] | 0.0017 | 0.0017 | 0.0017 | 0.0014 | 0.0014 | 0.0014 |
| r230 | atp[c] + amp[c] <=> 2 adp[c] | 0.0112 | 0.0112 | 0.0112 | 0.0081 | 0.0081 | 0.0081 |
| r231 | atp[c] + cmp[c] <=> adp[c] + cdp[c] | 0.0022 | 0.0022 | 0.0022 | 0.0018 | 0.0018 | 0.0018 |
| r232 | atp[c] + dcmp[c] <=> adp[c] + dcdp[c] | 0.0000 | 0.0000 | 0.0000 | 0.0000 | 0.0000 | 0.0000 |
| r233 | atp[c] + damp[c] <=> adp[c] + dadp[c] | −0.0017 | −0.0017 | −0.0017 | −0.0015 | −0.0015 | −0.0015 |
| r234 | atp[c] + dgmp[c] <=> adp[c] + dgdp[c] | 0.0000 | 0.0000 | 0.0000 | 0.0000 | 0.0000 | 0.0000 |
| r235 | atp[c] + gmp[c] <=> adp[c] + gdp[c] | 0.0000 | 0.0000 | 0.0000 | 0.0000 | 0.0000 | 0.0000 |
| r236 | atp[c] + cdp[c] <=> adp[c] + ctp[c] | 0.0022 | 0.0022 | 0.0022 | 0.0018 | 0.0018 | 0.0018 |
| r237 | atp[c] + dudp[c] <=> adp[c] + dutp[c] | 0.0000 | 0.0000 | 0.0000 | 0.0000 | 0.0000 | 0.0000 |
| r238 | atp[c] + gdp[c] <=> adp[c] + gtp[c] | 0.0012 | 0.0012 | 0.0012 | 0.0010 | 0.0010 | 0.0010 |
| r239 | atp[c] + udp[c] <=> adp[c] + utp[c] | 0.0002 | 0.0002 | 0.0002 | 0.0002 | 0.0002 | 0.0002 |
| r240 | pi[c] + adn[c] <=> r1p[c] + ade[c] | −0.0017 | −0.0017 | −0.0017 | −0.0014 | −0.0014 | −0.0014 |
| r241 | pi[c] + dad-2[c] <=> 2dr1p[c] + ade[c] | 0.0017 | 0.0017 | 0.0017 | 0.0014 | 0.0014 | 0.0014 |
| r242 | adp[c] + trdrd[c] -> h2o[c] + trdox[c] + dadp[c] | 0.0017 | 0.0017 | 0.0017 | 0.0015 | 0.0015 | 0.0015 |
| r243 | trdrd[c] + cdp[c] -> h2o[c] + trdox[c] + dcdp[c] | 0.0000 | 0.0000 | 0.0000 | 0.0000 | 0.0000 | 0.0000 |
| r244 | trdrd[c] + gdp[c] -> h2o[c] + trdox[c] + dgdp[c] | 0.0000 | 0.0000 | 0.0000 | 0.0000 | 0.0000 | 0.0000 |
| r245 | trdrd[c] + utp[c] -> h2o[c] + trdox[c] + dutp[c] | 0.0000 | 0.0000 | 0.0000 | 0.0000 | 0.0000 | 0.0000 |

(*continued on next page*)

**Table 3** (*continued*)

| Reaction name | Reaction | Steady-state 1 | | | Steady-state 2 | | |
|---|---|---|---|---|---|---|---|
| | | Optimal flux (mol/CmolX/h) | Minimum flux (mol/CmolX/h) | Maximum flux (mol/CmolX/h) | Optimal flux (mol/CmolX/h) | Minimum flux (mol/CmolX/h) | Maximum flux (mol/CmolX/h) |
| r246 | mlthf[c] + dump[c] -> dhf[c] + dtmp[c] | 0.0000 | 0.0000 | 0.0000 | 0.0000 | 0.0000 | 0.0000 |
| r247 | atp[c] + ump[c] <=> adp[c] + udp[c] | 0.0002 | 0.0002 | 0.0002 | 0.0002 | 0.0002 | 0.0002 |
| r248 | atp[c] + dump[c] <=> adp[c] + dudp[c] | 0.0000 | 0.0000 | 0.0000 | 0.0000 | 0.0000 | 0.0000 |
| r249 | 25aics[c] <=> fum[c] + aicar[c] | 0.0004 | 0.0004 | 0.0004 | 0.0003 | 0.0003 | 0.0003 |
| r250 | asp-L[c] + gtp[c] + imp[c] -> 2 h[c] + pi[c] + gdp[c] + dcamp[c] | 0.0005 | 0.0005 | 0.0005 | 0.0004 | 0.0004 | 0.0004 |
| r251 | dcamp[c] <=> fum[c] + amp[c] | 0.0005 | 0.0005 | 0.0005 | 0.0004 | 0.0004 | 0.0004 |
| r252 | asp-L[c] + cbp[c] -> h[c] + pi[c] + cbasp[c] | 0.0003 | 0.0003 | 0.0003 | 0.0002 | 0.0002 | 0.0002 |
| r253 | atp[c] + h2o[c] + gln-L[c] + utp[c] -> adp[c] + 2 h[c] + pi[c] + glu-L[c] + ctp[c] | 0.0001 | 0.0001 | 0.0001 | 0.0001 | 0.0001 | 0.0001 |
| r254 | q8[c] + dhor-S[c] -> q8h2[c] + orot[c] | 0.0003 | 0.0003 | 0.0003 | 0.0002 | 0.0002 | 0.0002 |
| r255 | h2o[c] + dhor-S[c] <=> h[c] + cbasp[c] | −0.0003 | −0.0003 | −0.0003 | −0.0002 | −0.0002 | −0.0002 |
| r256 | h2o[c] + gln-L[c] + prpp[c] -> ppi[c] + glu-L[c] + pram[c] | 0.0004 | 0.0004 | 0.0004 | 0.0003 | 0.0003 | 0.0003 |
| r257 | atp[c] + h2o[c] + gln-L[c] + xmp[c] -> 2 h[c] + ppi[c] + amp[c] + glu-L[c] + gmp[c] | 0.0002 | 0.0002 | 0.0002 | 0.0002 | 0.0002 | 0.0002 |
| r258 | h2o[c] + imp[c] <=> fprica[c] | −0.0007 | −0.0007 | −0.0007 | −0.0006 | −0.0006 | −0.0006 |
| r259 | nad[c] + h2o[c] + imp[c] -> h[c] + nadh[c] + xmp[c] | 0.0002 | 0.0002 | 0.0002 | 0.0002 | 0.0002 | 0.0002 |
| r260 | ppi[c] + orot5p[c] <=> prpp[c] + orot[c] | −0.0003 | −0.0003 | −0.0003 | −0.0002 | −0.0002 | −0.0002 |
| r261 | h[c] + orot5p[c] -> co2[c] + ump[c] | 0.0003 | 0.0003 | 0.0003 | 0.0002 | 0.0002 | 0.0002 |
| r262 | atp[c] + hco3[c] + air[c] -> adp[c] + h[c] + pi[c] + 5caiz[c] | 0.0004 | 0.0004 | 0.0004 | 0.0003 | 0.0003 | 0.0003 |
| r263 | 5aizc[c] <=> 5caiz[c] | −0.0004 | −0.0004 | −0.0004 | −0.0003 | −0.0003 | −0.0003 |
| r264 | atp[c] + fpram[c] -> adp[c] + 2 h[c] + pi[c] + air[c] | 0.0004 | 0.0004 | 0.0004 | 0.0003 | 0.0003 | 0.0003 |
| r265 | aicar[c] + 10fthf[c] <=> thf[c] + fprica[c] | 0.0007 | 0.0007 | 0.0007 | 0.0006 | 0.0006 | 0.0006 |
| r266 | atp[c] + asp-L[c] + 5aizc[c] <=> adp[c] + h[c] + pi[c] + 25aics[c] | 0.0004 | 0.0004 | 0.0004 | 0.0003 | 0.0003 | 0.0003 |
| r267 | atp[c] + h2o[c] + gln-L[c] + fgam[c] -> adp[c] + h[c] + pi[c] + glu-L[c] + fpram[c] | 0.0004 | 0.0004 | 0.0004 | 0.0003 | 0.0003 | 0.0003 |
| r268 | 10fthf[c] + gar[c] <=> h[c] + thf[c] + fgam[c] | 0.0004 | 0.0004 | 0.0004 | 0.0003 | 0.0003 | 0.0003 |
| r269 | atp[c] + gly[c] + pram[c] <=> adp[c] + h[c] + pi[c] + gar[c] | 0.0004 | 0.0004 | 0.0004 | 0.0003 | 0.0003 | 0.0003 |
| r278 | q8[c] + glyc3p[c] -> dhap[c] + q8h2[c] | 0.0000 | 0.0000 | 0.0000 | 0.0000 | 0.0000 | 0.0000 |
| r283 | atp[c] + coa[c] + ac[c] -> accoa[c] + ppi[c] + amp[c] | 0.0015 | 0.0015 | 0.0015 | 0.0000 | 0.0000 | 0.0000 |

(*continued on next page*)

**Table 3** (*continued*)

| Reaction name | Reaction | Steady-state 1 | | | Steady-state 2 | | |
|---|---|---|---|---|---|---|---|
| | | Optimal flux (mol/CmolX/h) | Minimum flux (mol/CmolX/h) | Maximum flux (mol/CmolX/h) | Optimal flux (mol/CmolX/h) | Minimum flux (mol/CmolX/h) | Maximum flux (mol/CmolX/h) |
| Protein_ amino_acids | 0.113 ala-L[c] + 0.0532 asp-L[c] + 0.0532 asn-L[c] + 0.0599 glu-L[c] + 0.0259 met-L[c] + 0.0512 arg-L[c] + 0.0599 gln-L[c] + 0.0416 pro-L[c] + 0.0176 cys-L[c] + 0.0501 ser-L[c] + 0.0872 gly[c] + 0.0182 his-L[c] + 0.0605 lys-L[c] + 0.0545 thr-L[c] + 0.035 phe-L[c] + 0.0114 trp-L[c] + 0.029 tyr-L[c] + 0.0493 ile-L[c] + 0.0541 leu-L[c] + 0.0752 val-L[c] -> Aaprot[c] | 0.0165 | 0.0165 | 0.0165 | 0.0138 | 0.0138 | 0.0138 |
| Protein_ translation | 4 atp[c] + 3 h2o[c] + Aaprot[c] -> 4 adp[c] + 4 h[c] + 4 pi[c] + 4.77 Biom_Prot[c] | 0.0153 | 0.0153 | 0.0153 | 0.0128 | 0.0128 | 0.0128 |
| DNA | 2 atp[c] + h2o[c] + 0.246 damp[c] + 0.254 dcmp[c] + 0.254 dgmp[c] + 0.246 dtmp[c] -> 2 adp[c] + 2 h[c] + 2 pi[c] + 9.75 DNA[c] | 0.0001 | 0.0001 | 0.0001 | 0.0001 | 0.0001 | 0.0001 |
| RNA | 2 atp[c] + h2o[c] + 0.262 amp[c] + 0.2 cmp[c] + 0.216 ump[c] + 0.322 gmp[c] -> 2 adp[c] + 2 h[c] + 2 pi[c] + 9.58 RNAtot[c] | 0.0006 | 0.0006 | 0.0006 | 0.0005 | 0.0005 | 0.0005 |
| ETC_O2 | 2.98 h[c] + q8h2[c] + 0.5 o2[c] -> 2.98 h[e] + h2o[c] + q8[c] | 0.1909 | 0.1909 | 0.1909 | 0.1321 | 0.1321 | 0.1321 |
| ETC_NADH | 3.98 h[c] + nadh[c] + q8[c] -> 2.98 h[e] + nad[c] + q8h2[c] | 0.1623 | 0.1623 | 0.1623 | 0.1178 | 0.1178 | 0.1178 |
| ETC_FOR | 2.49 h[c] + q8[c] + for[c] -> 1.49 h[e] + co2[c] + q8h2[c] | 0.0020 | 0.0020 | 0.0020 | 0.0000 | 0.0000 | 0.0000 |
| LeanBiomass | 0.011447 glyc[c] + 0.000888 glycogen[c] + 0.000747 ptrc[c] + 0.000157 spmd[c] + 0.002838 hdca[c] + 0.002201 hdcea[c] + 0.001436 ocdcea[c] + 0.010214 etha[c] + 5.1e-05 lps_EC[c] + 0.000145 peptido_EC[c] + 0.692337 Biom_Prot[c] + 0.008103 DNA[c] + 0.050081 RNAtot[c] -> BuildingBlocks | 0.0000 | 0.0000 | 0.0000 | 0.0000 | 0.0000 | 0.0000 |
| EX_Biomass | Biomass -> | 0.1112 | 0.1112 | 0.1139 | 0.0932 | 0.0932 | 0.0980 |
| EX_sucrose[e] | sucrose[e] -> | −0.0180 | −0.0180 | −0.0180 | −0.0151 | −0.0151 | −0.0151 |
| EX_HB[c] | HB[c] -> | 0.0001 | 0.0001 | 0.0001 | 0.0016 | 0.0016 | 0.0016 |
| SucroseSimporter | h[e] + sucrose[e] -> *h*[c] + sucrose[c] | 0.0180 | 0.0180 | 0.0180 | 0.0151 | 0.0151 | 0.0151 |
| SucroseHydrolase | h2o[c] + sucrose[c] -> fru[c] + glucose[c] | 0.0180 | 0.0180 | 0.0180 | 0.0151 | 0.0151 | 0.0151 |

(*continued on next page*)

**Table 3** (*continued*)

| Reaction name | Reaction | Steady-state 1 | | | Steady-state 2 | | |
|---|---|---|---|---|---|---|---|
| | | Optimal flux (mol/CmolX/h) | Minimum flux (mol/CmolX/h) | Maximum flux (mol/CmolX/h) | Optimal flux (mol/CmolX/h) | Minimum flux (mol/CmolX/h) | Maximum flux (mol/CmolX/h) |
| FruKin | atp[c] + fru[c] -> f6p[c] + adp[c] + *h*[c] | 0.0180 | 0.0180 | 0.0180 | 0.0151 | 0.0151 | 0.0151 |
| GluKin | atp[c] + glucose[c] -> g6p[c] + adp[c] + *h*[c] | 0.0180 | 0.0180 | 0.0180 | 0.0151 | 0.0151 | 0.0151 |
| sintPHB | h[c] + nadh[c] + 2 accoa[c] -> nad[c] + 2 coa[c] + HB[c] | 0.0001 | 0.0001 | 0.0001 | 0.0016 | 0.0016 | 0.0016 |
| Plasmid | 2 atp[c] + h2o[c] + 0.228 damp[c] + 0.272 dcmp[c] + 0.272 dgmp[c] + 0.228 dtmp[c] -> 2 adp[c] + 2 h[c] + 2 pi[c] + 9.75 Plasmid | 0.0000 | 0.0000 | 0.0000 | 0.0000 | 0.0000 | 0.0000 |
| RecombinantP | 4 atp[c] + 3 h2o[c] + Aaprot[c] -> 4 adp[c] + 4 h[c] + 4 pi[c] + 4.77 RP | 0.0012 | 0.0012 | 0.0012 | 0.0010 | 0.0010 | 0.0010 |
| Joining_Building_Blocks | 0.010852 glyc[c] + 0.000842 glycogen[c] + 0.000709 ptrc[c] + 0.000149 spmd[c] + 0.002691 hdca[c] + 0.002086 hdcea[c] + 0.001362 ocdcea[c] + 0.009683 etha[c] + 4.8e-05 lps_EC[c] + 0.000138 peptido_EC[c] + 0.656327 Biom_Prot[c] + 0.007682 DNA[c] + 0.047476 RNAtot[c] + 0.000946 Plasmid + 0.050939 RP -> BuildingBlocksBurden | 0.1112 | 0.1112 | 0.1112 | 0.0932 | 0.0932 | 0.0932 |
| Biomass_Formation | 0.46 atp[c] + 0.46 h2o[c] + BuildingBlocksBurden -> 0.46 adp[c] + 0.46 h[c] + 0.46 pi[c] + Biomass | 0.1112 | 0.1112 | 0.1112 | 0.0932 | 0.0932 | 0.0932 |

To verify the ability of *phaB*$^{CAp}$ to encode for a protein capable to catalyze *in vivo* the conversion of acetoacetyl-CoA to 3-hydroxybutyryl-CoA, an artificial operon was constructed joining the genes *phaC* and *phaA* from *C. necator* (encoding for a PHB synthase and a $\beta$-ketothiolase respectively) and *phaB*$^{CAp}$. The fragment embracing the open reading frames of *phaCA* genes plus the intergenic space between *phaA* and *phaB* (including the Shine-Dalgarno sequence upstream of *phaB*) from *C. necator* was amplified from the plasmid pBBRMCS-2-phaCABCnecator using the primers phaCABRalsXhoUPCrt and phaPCARalsBamDwCrt. After restriction (*Xho*I and *BamH*I) of the PCR product, it was cloned into the pTrcMCS vector to obtain the resultant plasmid pTrc-phaCACnecator. Then, *phaB*$^{CAp}$ was amplified from the plasmid pMiniT-phaB$^{CAp}$ using the primers phaB-PAO-nat_Bam2.FOR and phaBPAOHind.REV. The obtained PCR product was restricted (*BamH*I and *Hind*III) and ligated downstream of the fragment *phaCA* in pTrc-phaCACnecator. The obtained plasmid was named pTrc-phaCACnecatorphaBCAp. Finally, a fragment embracing the genes phaCA$^{Cnecator}$phaB$^{CAp}$ was amplified using the primers phaCABRals_NdeUpCrt and PAOphaB_XhoDwCrt, restricted with *Nde*I and *Xho*I, and ligated into the pCOLA-duet vector. The resultant plasmid was named pCola-phaCACnecatorphaBCAp and carried the artificial operon phaCA$^{Cnecator}$phaB$^{CAp}$ under the control of the T7 promoter.

Finally, to avoid the use of antibiotics in the planned continuous cultures, we transferred the genes *cscB, cscK* and *cscA* from *E. coli* W to the plasmid pCola-phaCACnecatorphaBCAp. The *cscABK* genes encodes for the sucrose hydrolase, the sucrose:proton symporter and the fructose kinase from *E. coli* W, respectively. *E. coli* strains from the K-12 group are naturally unable to grow on sucrose as the sole carbon source, but the introduction of *cscABK* genes confers this ability [8]. Therefore, the resultant plasmid with the genes *cscB, cscK, cscA, phaC, phaA* and *phaB* becomes essential for the growth of an *E. coli* K-12 derived strain on sucrose as the sole carbon source. The resultant plasmid was named pColaphaCABcscABK. For its construction, a DNA fragment embracing the genes *cscB, cscK, cscA* was amplified by PCR using as the template genomic DNA from *E. coli* W and the primers XhoIcrtcscBFW and cscAXhoIcrtRV. The resultant PCR product was restricted with the enzyme *Xho*I and ligated into the plasmid pColaphaCACnecatorphaBCAp, who was previously restricted also with *Xho*I and treated with alkaline phosphatase to minimizes recircularization.

After transformation and plasmid propagation in *E. coli* One Shot® TOP10, the plasmid pColaphaCABcscABK was purified and introduced, by electroporation, in cells of the *E. coli* strain MG1655(DE3)$\Delta$5, kindly donated by professor Isabel Rocha (CEB-Centre of Biological Engineering, University of Minho, Portugal). That strain was previously modified to express the T7 RNA polymerase upon induction with Isopropyl $\beta$-D-1-thiogalactopyranoside (IPTG) [9]; and its genes *adhE, adhP, ldhA, pta* and *mhpF* were previously deleted.

The DNA sequence maps of all the plasmids involved in this research project can be found in the repository "**NADH-driven polyhydroxybutyrate accumulation in *E. coli* dataset 2**″ in Mendeley Data.

### 2.2. Protein purification

Cells of *E. coli* BL21(DE3) transformed with the plasmid pCOLA-His-phaBCAp6 and pColaphaB-Chimera were aerobically grown on LB supplemented with Kanamycin (180 rpm, 37 °C) up to an optical density (600 nm) of 0.5. Over-expression of AAR$^{CAp}$ and AAR$^{Chimera}$ was induced with IPTG 200 (0.5 mM) and temperature was decreased to 25 °C. Induced cultures were grown for 16 h and the cells were harvested by centrifugation (2500 g, 4 °C, 20 min). To wash the cells, the resultant pellets were suspended in ice-cold Buffer A (50 mM Tris, 100 mM NaCl, 5 mM $MgCl_2$, pH 8) up to 10% of the original culture volume and centrifuged (2500 g, 4 °C, 10 min). The resultant pellets were suspended again in 10% of the original culture volume using ice-cold Buffer A but supplemented with DL-Dithiothreitol 2 mM and cOmplete$^{TM}$ EDTA-free Protease Inhibitor Cocktail (Roche) prepared according with the instructions of the manufacturer. Cells were broken by sonication and the cell-free extracts were obtained rescuing the supernatant after centrifugation (45 min, 4 °C, 15,000 g). The His-tagged proteins were purified from the obtained

cell-free extracts using 5 ml HisTrap FF columns (GE Healthcare), following the instructions of the manufacturer. Buffer A supplemented with a basal concentration of imidazole (20 mM) and NaCl (100 mM) was employed to equilibrate the columns. The obtained cell-free extracts were spiked with NaCl and imidazole to achieve the same concentration present in the equilibration buffer. After the cell-free extracts were loaded, columns were washed with equilibration buffer, passing through them at least 20 times the volume of the loaded cell-free extracts. For the elution of his-tagged proteins, volumes of buffer A equivalent to 20 times the loaded cell-free extracts were injected in the columns, but buffer A was supplemented with a steadily increasing concentration of imidazole, conforming a gradient from 20 mM to 500 mM. Fractions of 2 ml were harvested in Eppendorf tubes. The NADH-linked acetoacetyl-CoA reductase activities were spectrophotometrically measured in the fractions (NADH 100 $\mu$M, acetoacetyl-CoA 100 $\mu$M in buffer A). Those fractions with acetoacetyl-CoA reductase activities ranking in the upper quartile were pooled. Imidazole was washed out from the pools and proteins were concentrated by centrifugation using a Millipore® Amicon® Ultra-Centifugal Filter Concentrator with a cut-off of 10 kDa. The resultant pools were stored at −20 °C, with 50% glycerol, until perform the enzymatic assays. The purity of the obtained protein samples was assessed by SDS-PAGE.

### 2.3. Enzymatic assays

The substrates employed for the enzymatic assays were purchased from Sigma (NADH and NADPH) and Santa Cruz Biotechnology (acetoacetyl-CoA) and had analytical grade quality. NADH and NADPH were freshly prepared by dissolving them in Buffer A. Acetoacetyl-CoA, $NAD^+$ and $NADP^+$ were freshly dissolved in des-ionized water (resistivity 18.2 MΩ*cm at 25 °C). Substrate concentration in these stock solutions was estimated by spectrophotometry, dissolving samples taken from the stocks in 50 mM MOPS (pH 7), 5 mM $MgCl_2$, 5 mM NaCl. The concentrations of the resultant solutions were determined by spectrophotometry, using apparent molar extinction coefficients obtained in conditions similar to ours ($\varepsilon^{app}$ at 340 nm for NAD(P)$H = 6220\,M^{-1}\,cm^{-1}$; for acetoacetyl-CoA at 310 nm, $\varepsilon^{app} = 11{,}000\,M^{-1}\,cm^{-1}$). The protein concentration was determined using the Protein assay reagent (Bio-Rad) and Bovine Serum Albumin (Bio-Rad) as standard.

To calculate the acetoacetyl-CoA reductase activity, the consumption of acetoacetyl-CoA and NAD(P)H was monitored following the changes in the absorbances at 310 nm or 360 nm. The apparent molar extinction coefficients were $\varepsilon^{AcAcCoA,310} = 11{,}000\,M^{-1}\,cm^{-1}$, $\varepsilon^{NAD(P)H,310} = 3340\,M^{-1}\,cm^{-1}$, $\varepsilon^{AcAcCoA,360} = 900\,M^{-1}\,cm^{-1}$, and $\varepsilon^{NAD(P)H,360} = 4275\,M^{-1}\,cm^{-1}$. We did not register the changes in absorbance at 340 nm to avoid optical artefacts.

Initial rates and reaction progress curves were studied in the Buffer A at 30 °C. All the spectrophotometric measurements were performed in a Biotek Synergy HTX plate reader, using the in-build path length correction option to estimate the heights of the columns of liquid where the reactions happened. To estimate the initial rates estimations, pseudo-linear temporal changes in the absorbance were considered inside the time frame where less than 5% of the substrate had been consumed.

### 2.4. Analysis of the kinetic data

The reactions catalyzed by acetoacetyl-CoA reductases (E.C. 1.1.1.36) are bi-substrate bi-product (BiBi) reactions. However, for the kinetic parameter estimation, those BiBi reactions were modeled as pseudo-mono-substrate mono-product reactions. The initial concentration of the substrate not explicitly considered in each experiment is reported in each case.

Parameter estimations were performed with the software DYNAFIT [1]. For the analysis of initial rates, a simple Michaelian model (rapid-equilibrium) was assumed. Reaction progress curves were analyzed with steady-state models. DYNAFIT enables to do global fittings, i.e., it fits simul-

taneously data obtained using different concentrations of substrate and/or enzyme and/or modifiers. DYNAFIT enables to find the best fitted values for the parameters of a given model and it also enables to compare different models, finding which model best explains the observed results (model discrimination).

When modeling with DYNAFIT, it is not necessary to know the rate equation describing the chemical reaction(s) under study. What the user must provide is a (bio)chemical mechanism representing the meaningful interactions. For example, product inhibition can be mechanistically represented in the following way, where $k_1$, $k_{-1}$, $k_{off}$ and $k_{cat}$ are the rate constants characterizing the elemental interactions:

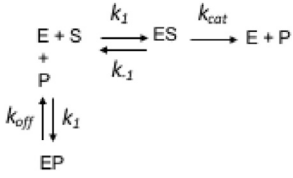


This mechanism can be written in DYNAFIT code as follows:

```
E + S <===> ES : k1 kminus1 ;                    (1)

ES - - > E + P : kcat ;                          (2)

E + P <===> EP : k1 koff ;                       (3)
```

The semicolon (;) is used in DYNAFIT to comment the lines. Therefore, in a line, DYNAFIT is "blind" to everything written after the symbol ";".

Note that rate constant $k_1$ could have different values in the elemental interaction (1) and in the elemental interaction (3). Why using the same constant $k_1$? We have four unknown parameters ($k_1$, $k_{-1}$, $k_{off}$ and $k_{cat}$) to describe three chemical transformations. To solve this mathematical problem, an arbitrary value could be assigned to $k_1$. Certainly, the best fitted values for $k_{-1}$ and $k_{off}$ obtained by this method will be arbitrary as well, but they are not independent of the arbitrary value assigned to $k_1$.

Anyways, for many practical applications, it is enough to know the constants $K_M$, $K_i$ and $k_{cat}$. The kinetic constants $K_M$ and $K_i$ are more or less complex functions of elemental rate constants, depending on the mechanism. For the specific case of product inhibition shown in the scheme above, $K_M$ and $K_i$ are defined as:

$$K_M = \frac{k_{-1} + k_{cat}}{k_1}$$

$$K_i = \frac{k_{off}}{k_1}$$

The enzyme stability tests showed that partial enzyme inactivation could happen. Therefore, in the analysis of the reaction progress curves, enzyme degradation was considered. It was modeled as a first order decay process:

```
E - -> InactiveE    : kdeg
```

The value of the degradation constant ($k_{deg}$) was estimated by DYNAFIT.

The required scripts are provided in the repository "**NADH-driven polyhydroxybutyrate accumulation in *E.coli* dataset 2**" in Mendeley Data. To run these scripts, it is necessary to **download** and activate DYNAFIT (freely available for academic institutions). Note that DYNAFIT scripts contain a line indicating the route to the data containing folder. These are the data that will be processed by the script. This route is usually written with reference to the folder where DYNAFIT itself is installed (annotated as ./). For example, in the script to analyze the data corresponding

to the experiment named "AARCAp_varying_AcAcCoA_NADH", it is possible to find the following lines (function of each line is commented after the semicolon):

[*data*]; keyword in DYNAFIT announcing the section where data will be declared
directory ./results/VovsS/AARCAp;data are in folder AARCAP, inside folder VovsS, inside the folder results, placed in the same folder where DYNAFIT was installed.
extension txt; indicates that the data are in a ".txt" file
variable S; indicates that the independent variable is the substrate concentration, represented in the chemical mechanism as S
file data; indicates that the file with the experimental data is named "data.txt"
[*output*]; keyword in DYNAFIT announcing the section dealing with the results of the analyses
directory ./results/VovsS/AARCAp/output1; indicates that the folder named "output1" will be created in this route

Another important information contained in DYNAFIT scripts is the so called "Response". The Response or molar Response is a proportionality constant to express the output parameters in convenient units. In this specific case, we were interested in expressing the values of $K_M$ and $K_i$ in micromolar ($\mu$M) and the values of $k_{cat}$ in micromole of product generated, per micromole of active sites, per second ($s^{-1}$ for simplicity). In the case of the progress curves, in the input files, the concentration of the substrate was already in units of micromolar and the time was in seconds. Therefore, the molar Response in the scripts was $S = 1$.

In the case of initial rates versus substrate concentrations, the initial rates were expressed in units of micromolProduct(Substrate)/micromolEnzyme/s, then the molar response was $P = 1$. On the other hand, if the initial rates were in units of micromolP/mgEnzyme/min (U/mg), then it would be necessary to calculate the conversion factor. Considering the molecular weight of the poly-histidine-tagged form of the protein encoded by $phaB^{CAp}6$ (27,554 g/mol), the molar Response would be:

$$\frac{1\ \mu mol_{product}}{mg_{enzyme} * min} = \frac{1\ \mu mol_{product}}{\frac{10^{-3} g_{enzyme} * \ 10^{6}\ \mu mol_{enzyme}}{27554\ g_{enzyme}} * 60\ s} = 0.459\ s^{-1}$$

These instructions should be enough to run the scripts with DYNAFIT. However, for better understanding of all the lines in the scripts, and eventually modify these scripts for other applications, we strongly recommend to check the DYNAFIT scripting rules, freely available in the website of the developer (http://www.biokin.com/dynafit/).

Estimation of the relative cofactor usage and flux capacity of a reaction catalyzed by an acetoacetyl-CoA reductase

To quantify the relative use of NADH over NADPH (or vice versa) by a given acetoacetyl-CoA reductase, we calculated the ratio of the activities with NADH and NADPH. These activities were calculated adapting a generic BiBi equation described by Rohwer and co-workers [10] to the reactions catalyzed by acetoacetyl-CoA reductases:

$$v^{NADH} = \frac{k_{cat}^{NADH} * E * \frac{NADH * AcAcCoA}{K^{NADH} * K^{AcAcCoA}} * \left(1 - \frac{NAD * 3HBCoA}{NADH * AcAcCoA * K_{eq}}\right)}{\left(1 + \frac{NADH}{K^{NADH}} + \frac{3HBCoA}{K^{3HBCoA}}\right) * \left(1 + \frac{AcAcCoA}{K^{AcAcCoA}} + \frac{NAD}{K^{NAD}}\right)}.$$

where $K^{NADH}$, $K^{AcAcCoA}$, $K^{3HBCoA}$ and $K^{NAD}$ are dissociation constants associated to the interactions between the corresponding ligands and different forms of the enzyme. The experimentally determined $K_M$ and $K_{ic}$ were considered good approximations of the dissociation constants of the generic equation. The constants not directly available from our experimental data were estimated taking advantage of the Haldane relationships.

Another important detail was the consideration of NADPH and $NADP^+$ as competitive inhibitors of NADH and $NAD^+$binding. This way, the terms $K^{NADH}$ and $K^{NAD}$ were multiplied by the factor $(1 + NADPH/K^{NADPH} + NADP/K^{NADP})$. A similar analysis was applied to the reactions catalyzed by NADPH.

Different to other approaches, we considered the cofactor specificity as a dynamic property, i.e., it is not a fixed value, it changes depending on the $NAD^+$, NADH, $NADP^+$ and NADPH concentrations. With the scripts available in the repository "NADH-driven polyhydroxybutyrate accumulation in E. coli dataset 2″ in Mendeley Data, individual $NAD^+$, NADH, $NADP^+$ and NADPH concentrations are calculated by solving a simple system of algebraic equations. These equations reflect two physiologically relevant principles: (i) cofactor concentrations have to fulfill the thermodynamic constraints enabling the operation of the Embden-Meyerhof pathway and (ii) the concentration sums ($NAD^+ + NADH$) and ($NADP^+ + NADPH$) were considered conserved moieties.

It should be noticed that the ratios of the activities with NADH and NADPH $R = v^{NADH}/v^{NADPH}$ is independent of the enzyme concentration because the terms "E" in the numerator and denominator cancel each other. On the other hand, the flux capacity does depends on the enzyme ($AAR^{CAp}$) concentration, and this dependency is linear:

$$Flux\ capacity = \frac{k_{cat}^{NADH} * AAR^{CAp} * \frac{NADH*AcAcCoA}{K^{NADH}*\left(1+\frac{NADPH}{K^{NADPH}}+\frac{NADP}{K^{NADP}}\right)*K_{NADH}^{AcAcCoA}} * \left(1-\frac{NAD*3HBCoA}{NADH*AcAcCoA*K_{eq}}\right)}{\left(1+\frac{NADH}{K^{NADH}*\left(1+\frac{NADPH}{K^{NADPH}}+\frac{NADP}{K^{NADP}}\right)}+\frac{3HBCoA}{K_{NADH}^{3HBCoA}}\right)*\left(1+\frac{AcAcCoA}{K_{NADH}^{AcAcCoA}}+\frac{NAD}{K^{NAD}*\left(1+\frac{NADPH}{K^{NADPH}}+\frac{NADP}{K^{NADP}}\right)}\right)}$$

Therefore, besides the kinetic parameters and the ligands concentrations, enzyme concentration is required. If the kinetic parameters of the enzyme are known, it is possible to have an estimate of the enzyme concentration using as input an initial rate measured in defined conditions. During our initial rate measuring, the concentrations of the products were negligible, and the competitors $NADP^+$ and NADPH were not present; therefore, the generic equation can be simplified to:

$$initial\ rate = \frac{k_{cat}^{NADH} * AAR^{CAp} * \frac{NADH*AcAcCoA}{K^{NADH}*K^{AcAcCoA}}}{\left(1+\frac{NADH}{K^{NADH}}\right)*\left(1+\frac{AcAcCoA}{K^{AcAcCoA}}\right)}$$

With concentrations of acetoacetyl-CoA 50 $\mu$M and NADH 50 $\mu$M, an initial rate of specific acetoacetyl-CoA reductase activity of 11.3 nmol/min/mg_cytoplasmic_proteins was measured in cell-free extracts from the engineered *E. coli* strain (((F– λ– *ilvG*– *rfb*-50 *rph*-1 (DE3) Δ*adhE* Δ*adhP* Δ*ldhA* Δ*pta* Δ*mhpF*)) transformed with the plasmid pCOLA-phaCAphaB-cscABK. With these data, enzyme concentration was estimated:

$$AAR^{CAp} = \frac{initial\ rate*K_M^{NADH}*K_M^{AcAcCoA}*\left(1+\frac{NADH}{K_M^{NADH}}\right)*\left(1+\frac{AcAcCoA}{K_M^{AcAcCoA}}\right)}{k_{cat}*NADH*AcAcCoA} = 0.00135\ \frac{mg\ AAR^{CAp}}{mg\ cytoplasmic\ protein}$$

where, $k_{cat} = 8.9$ mol NADH/mol_$AAR^{CAp}$/s; NADH in the assay = 50 µM; AcAcCoA in the assay = 50 µM; $K_M{}^{NADH} = 7.7$ µM; $K_M{}^{AcAcCoA} = 56.7$ µM; Molecular weight $AAR^{CAp}$ = 25,896 gr_$AAR^{CAp}$/mol_$AAR^{CAp}$; acetoacetyl-CoA reductase specific activity = 11 nmol NADH/min/mg_cytoplasmic_protein.

Using the appropriate conversion factors, this enzyme abundancy can be expressed in units of mol $AAR^{CAp}$ per gram of cell dry weight:

$$\frac{0.00135\ g\ AAR^{CAp}}{g\ cyt.\ protein} * \frac{1\ mol\ AAR^{CAp}}{25896\ g\ AAR^{CAp}} * \frac{0.8\ g\ cyt.\ protein}{1\ g\ total\ protein} * \frac{0.68\ g\ total\ protein}{1\ gCDW} = 0.0283\ \frac{\mu mol\ AAR^{CAp}}{gCDW}$$

Finally, converting micromole to millimole, and second to hours; the flux capacity can be expressed in units of mmol/gCDW/h.

Biomass composition of the engineered *E. coli* strain (((F– λ– *ilvG*– *rfb*-50 *rph*-1 (DE3) Δ*adhE* Δ*adhP* Δ*ldhA* Δ*pta* Δ*mhpF*)) transformed with the plasmid pCOLA-phaCAphaB-cscABK.

As reference for the lean biomass composition, we took the values reported by Taymaz-Nikerel and co-workers for *E. coli* K-12 MG1655 aerobically growing on glucose as the sole carbon source, at a dilution rate of 0.1 $h^{-1}$ [11]. Considering the elemental composition and the relative contributions to the weight of the different biomass components, we calculated: (1) the molar proportion of the different biomass components in the lean biomass, (2) the relative atomic composition of the total biomass ($C_1H_{1.681}N_{0.253}O_{0.3471}S_{0.0067}P_{0.0066}$), (3) the molecular weight of the virtual molecule representing the total biomass ($M_{wx} = 23.195$), and (4) the corresponding degree of reduction (4.301).

Given the fact that the genes enabling the PHB accumulation and the genes enabling the sucrose consumption were introduced via the plasmid pCOLA-phaCAphaB-cscABK, some modifications were introduced to the biomass composition to account for the plasmidial DNA and the heterologous proteins encoded by the genes carried by this plasmid.

To calculate the contribution of the plasmid to the cellular weight, some assumptions were done. In *E. coli*, it has been previously shown that the cell volume decreases with the dilution rate following a second degree polynomial equation [12]. Therefore, the published data of plasmid weights at different dilution rates [13] were fitted to a second degree polynomial equation to calculate the weight of the plasmids at 0.1 $h^{-1}$. The result was 0.0013 g_plasmid/gCDW (0.13%). Because available reports about the change in the copy number are contradictory, it was assumed that the number of plasmids per cell does not change with the dilution rate. The analyses of the GC content of the plasmid (54%) showed that the relative atomic composition of this molecule do not diverge significantly from the average *E. coli* chromosomal DNA. This way, the same relative atomic composition of the chromosomal DNA ($C_1H_{1.05}N_{0.385}O_{0.616}P_{0.103}$) was assigned for this plasmid.

On the other hand, to calculate the contribution to the cellular weight of the heterologous proteins encoded by the episomal genes carried by the plasmid, further assumptions were made. Because the DNA sequences of the episomal genes is known, it was possible to calculate the molecular weight of the encoded proteins. The contribution of the plasmid-encoded aminoglycoside acetyltransferase (KanR, protein responsible for resistance to kanamycin) to the *E. coli* proteome was calculated using the specific aminoglycoside acetyltransferase activities reported for *E. coli* C600 expressing the plasmid pWP701 and the activity of the aminoglycoside acetyltransferase purified from this strain [14]:

$$E = V^{max}/k_{cat} = (0.032\,\text{katal/mg\_cytoplasmic\_protein})/(2\,\text{katal/mg\_KanR})$$
$$= 0.0160\text{mg\_KanR/mg\_cytoplasmic\_protein}$$

Assuming that *cscABK* and *KanR* genes were expressed with similar strength, the relative contributions of the proteins encoded by the operon *cscABK* were calculated based on their molecular mass ratios respect to the molecular weight of the aminoglycoside acetyltransferase.

On the other hand, the specific $AAR^{CAp}$ activity measured in cells of the engineered strain under initial rates conditions (0.011 µmol NADH/min/mg_cytoplasmic_protein) was taken to calculate the contribution of this enzyme to the pool of cytoplasmic proteins, as explained above:

$$AAR = \frac{AAR\ sp.\ activity * K_M^{NADH} * K_M^{AcAcCoA} * \left(1 + \frac{NADH}{K_M^{NADH}}\right) * \left(1 + \frac{AcAcCoA}{K_M^{AcAcCoA}}\right)}{k_{cat} * NADH * AcAcCoA}$$
$$= 0.00135 \left(\frac{mgAAR}{mg\ cytoplasmic\ protein}\right)$$

Using the same approach applied to calculate the contributions to the proteome of the proteins encoded by the *cscABK* genes, the contributions of the proteins encoded by the $phaCA^{Cnecator}$ genes to the *E. coli* proteome were calculated considering their protein molecular mass ratios respect to the molecular weight of $AAR^{CAp}$. Knowning that around 80% of the *E. coli* proteome are soluble proteins and proteins constitute 68% of the cell dry weight, it was

**Table 4**
Contribution of the heterologous proteins to the biomass composition.

| | Elemental composition | | | | | | M (g/mol) | Individual contributions to cytoplasmic proteins pool |
|---|---|---|---|---|---|---|---|---|
| | C | H | N | O | S | P | | |
| KanR | 1387 | 2124 | 376 | 406 | 13 | 0 | 30,944 | 0.0160* |
| cscA | 2430 | 3619 | 685 | 707 | 21 | 0 | 54,353 | 0.0281* |
| cscB | 2249 | 3354 | 512 | 545 | 20 | 0 | 46,870 | 0.0242* |
| cscK | 1447 | 2305 | 407 | 442 | 17 | 0 | 32,983 | 0.0171* |
| phaB | 1142 | 1828 | 306 | 344 | 18 | 0 | 25,896 | 0.00135* |
| phaA | 1774 | 2906 | 502 | 538 | 21 | 0 | 40,502 | 0.0021* |
| phaC | 2900 | 4452 | 800 | 836 | 13 | 0 | 64,244 | 0.0033* |
| Sum of individual contributions | | | | | | | | 0.0920* |
| Protein content in Biomass (g_protein/gCDW) | | | | | | | | 0.6819 |
| Cytoplasmic proteins in total protein (%) | | | | | | | | 80 |
| contribution of heterologous protein to Biomass (g_heterologous_proteins/gCDW) | | | | | | | | 0.0502 |

* expressed in units of g_heterologous_protein/g_cytoplasmic_protein.

estimated that heterologous proteins should represent 0.0502 g/gCDW (5% of the cell dry weight) (Table 4).

The analyses of the elemental composition of the heterologous proteins pool ($C_1H_{1.515}N_{0.264}O_{0.279}S_{0.009}$) showed that it does not diverge significantly from the average *E. coli* chromosomally-encoded protein ($C_1H_{1.58}N_{0.288}O_{0.309}S_{0.009}$). This way, the same relative atomic composition of the chromosomally-encoded protein was assigned for the heterologous proteins pool.

Knowing the contributions of plasmid and heterologous proteins to the cellular weight, the contributions of other biomolecules were re-scaled. With the relative contributions of the lean biomass, the plasmid and the heterologous proteins to 1 gCDW of total biomass; and considering the relative atomic compositions of the lean biomass, the plasmid and the heterologous proteins, we calculated:

- The proportion between the virtual molecules representing the lean biomass, the plasmid and the heterologous proteins: 1 Lean Biomass: 0.0011 Plasmid: 0.0574 Heterologous proteins.
- The relative atomic composition of the biomass including plasmid and heterologous proteins ($C_1H_{1.6749}N_{0.255}O_{0.3453}S_{0.0069}P_{0.0063}$), the molecular weight of the virtual molecule representing the total biomass ($M_{wx} = 23.184$) and the corresponding degree of reduction (4.292).

The final result appears in Table 1. In the folder "Fermentations", in the repository "NADH-driven polyhydroxybutyrate accumulation in E. coli dataset 2″ in Mendeley Data, it is possible to find an Excel file named "Biomass composition" with all the above described calculations. Moreover, it is also possible to find a MATLAB script to generate an *in silico* metabolic model of the engineered strain.

It should be noticed that the bioenergetic parameters P/O ratio ($\delta$), growth dependent maintenance ($K_X$) and growth independent maintenance (mATP) are explicit (modifiable) in the script generating the *in silico* model, enabling the exploration of the effects of changing those parameters.

## Funding

This work was supported by the joint research program NWO (BRAZIL.2013.018) – FAPESP (2013/50,357-2). The contributions of Karel Olavarria and Mark C.M. van Loosdrecht were also supported by a SIAM Gravitation Grant (024.002.002) from the Netherlands Ministry of Education, Culture and Science (OCW) and NWO.

## Ethics Statement

Authors confirm that this article follows the ethical requirements established by Data in Brief and the Elsevier. This work does not involved the use of human subjects, animal experiments or data collected from social media platforms.

## Declaration of Competing Interest

The authors declare that they have no known competing financial interests or personal relationships which have or could be perceived to have influenced the work reported in this article.

## Data Availability

NADH-driven polyhydroxybutyrate accumulation in E. coli dataset 2 (Original data) (Mendeley Data)

## Supplementary Materials

Supplementary material associated with this article can be found in the online version at doi:10.1016/j.dib.2020.106588.

## CRediT authorship contribution statement

**Karel Olavarria:** Validation, Formal analysis, Investigation, Resources, Writing - original draft, Funding acquisition. **Caspar Quakkelaar:** Investigation. **Joachim van Renselaar:** Investigation. **Dennis Langerak:** Investigation. **Mark C.M. van Loosdrecht:** Supervision, Funding acquisition. **S.A. Wahl:** Supervision, Project administration, Funding acquisition.

## References

[1] P. Kuzmic, Program DYNAFIT for the analysis of enzyme kinetic data: application to HIV proteinase, Anal. Biochem. 237 (2) (1996) 260–273.
[2] B.D. Bennett, E.H. Kimball, M. Gao, R. Osterhout, S.J. Van Dien, et al., Absolute metabolite concentrations and implied enzyme active site occupancy in Escherichia coli, Nat. Chem. Biol. 5 (8) (2009) 593–599.
[3] M.R. de Graef, S. Alexeeva, J.L. Snoep, M.J Teixeira de Mattos, The steady-state internal redox state (NADH/NAD) reflects the external redox state and is correlated with catabolic adaptation in Escherichia coli, J. Bacteriol. 181 (8) (1999) 2351–2357.
[4] C. Chassagnole, N. Noisommit-Rizzi, J.W. Schmid, K. Mauch, M Reuss, Dynamic modeling of the central carbon metabolism of Escherichia coli, Biotechnol. Bioeng. 79 (1) (2002) 53–73.
[5] J. Schellenberger, R. Que, R.M.T. Fleming, I. Thiele, J.D. Orth, et al., Quantitative prediction of cellular metabolism with constraint-based models: the COBRA Toolbox v2.0, Nat. Protoc. 6 (9) (2011) 1290–1307.
[6] T. Maniatis, E.F. Fritsch, J Sambrook, Molecular cloning: a laboratory manual, Cold Spring Harbor, Cold Spring Harbor Laboratory, N.Y., 1982.
[7] G.J. Smolders, J. van der Meij, M.C. van Loosdrecht, J.J Heijnen, Model of the anaerobic metabolism of the biological phosphorus removal process: stoichiometry and pH influence, Biotechnol. Bioeng. 43 (6) (1994) 461–470.
[8] S. Sabri, J.A. Steen, M. Bongers, L.K. Nielsen, C.E Vickers, Knock-in/Knock-out (KIKO) vectors for rapid integration of large DNA sequences, including whole metabolic pathways, onto the Escherichia coli chromosome at well-characterised loci, Microb. Cell Fact. 12 (2013) 60.
[9] H.C. Tseng, C.H. Martin, D.R. Nielsen, K.L Prather, Metabolic engineering of Escherichia coli for enhanced production of (R)- and (S)-3-hydroxybutyrate, Appl. Environ. Microbiol. 75 (10) (2009) 3137–3145.
[10] J.M. Rohwer, A.J. Hanekom, C. Crous, J.L. Snoep, J.H Hofmeyr, Evaluation of a simplified generic bi-substrate rate equation for computational systems biology, Syst. Biol. 153 (5) (2006) 338–341.
[11] H. Taymaz-Nikerel, A.E. Borujeni, P.J. Verheijen, J.J. Heijnen, W.M van Gulik, Genome-derived minimal metabolic models for Escherichia coli MG1655 with estimated *in vivo* respiratory ATP stoichiometry, Biotechnol. Bioeng. 107 (2) (2010) 369–381.

[12] B. Volkmer, M. Heinemann, Condition-dependent cell volume and concentration of Escherichia coli to facilitate data conversion for systems biology modeling, PLoS One 6 (7) (2011) e23126.
[13] M.M. Ataai, M.L. Shuler, A mathematical model for prediction of plasmid copy number and genetic stability in Escherichia coli, Biotechnol. Bioeng. 30 (3) (1987) 389–397.
[14] B. Brau, W. Piepersberg, Purification and characterization of a plasmid-encoded aminoglycoside- (3)-N-acetyltransferase IV from Escherichia coli, FEBS Lett. 185 (1) (1985) 43–46.